without treatment of antibiotics and fasting was examined in reference to the AAR.

Measurement of H_2 concentration in the expired air of mice. Before surgery, expired H_2 concentrations were measured with an H_2 sensor (XP-3160; New Cosmos Electric, Osaka, Japan). Expired air of mice was forced to flow at 50 ml/min for 10 min into a gas-tight sampling bag made of aluminum. The expired air in the bag was then introduced into the H_2 sensor (Fig. 2*A*). We confirmed that the H_2 concentration in the expired air of antibiotics-treated mice was below the 1-ppm detection limit, whereas it was well over the detection limit in all of the antibiotics nontreated mice (Fig. 2*B*).

Echocardiography. Transthoracic echocardiography was performed with a commercially available echocardiography system (Pro-Sound SDD-4000; ALOKA, Tokyo, Japan), using a 4–14 MHz linear-array transducer. Closed-chest echocardiograms were obtained under anesthesia before the surgery and 24 h after reperfusion. The left ventricular ejection fraction (LVEF) was calculated using M-mode echocardiography.

Measurement of myocardial infarct size. At 24 h after reperfusion, the left coronary artery was religated, and a tissue-marking dye (Evans blue; Wako Pure Chemical, Tokyo, Japan) was injected through the inferior vena cava to determine the AAR. After the heart was harvested and placed in an agarose-containing well, the heart was sliced into 6 to 7 transverse slices of 1-mm thickness. The slices were placed in 1% 2,3,5-triphenyltetrazolium chloride solution in PBS for 10 min (first stain) and for 5 min (second stain), then washed with PBS for 5 min and fixed with formalin for 10 min. The infarct zone remained pale yellow, whereas the viable areas stained deep red. Digital images of the slices were obtained. The area stained with neither Evans blue (AAR) nor 2,3,5-triphenyltetrazolium chloride (infarct size) was measured on each slice image using an image software (ImageJ; National Institutes of Health) and summed. Ratios of AAR to the total area of the LV and the infarct size to AAR (infarct size/AAR) were calculated.

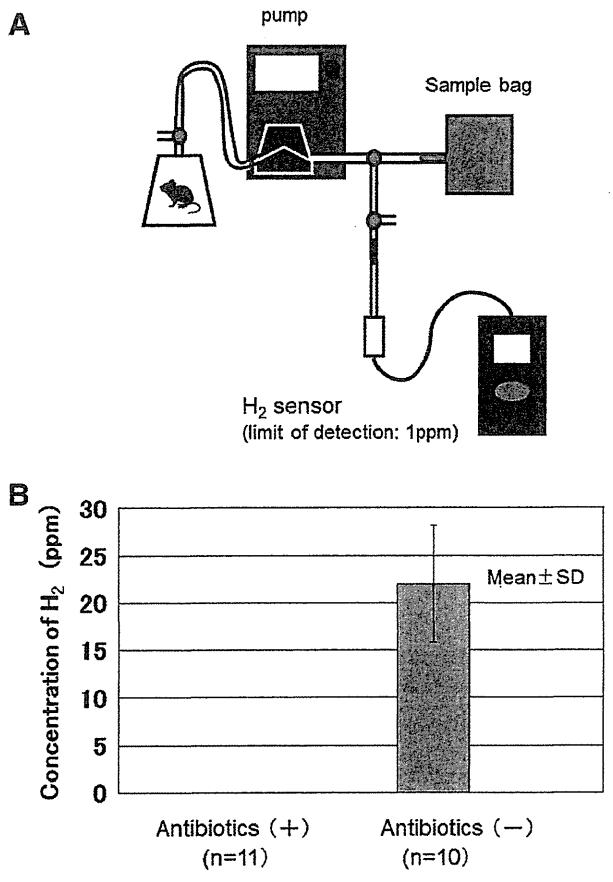

Fig. 2. Measurement of H_2 concentration in the expired air of mice. *A*: mice were placed in a cage of 500 ml. Expired air of mice was forced to flow at 50 ml/min into a sampling bag for 10 min. *B*: concentration of H_2 in expired air of mice, which were given antibiotics and were treated with fasting, decreased under the limit of detection.

Immunohistochemical staining. Immunohistochemical staining of the heart tissues for 8-hydroxy-2′-deoxyguanosine (8-OHdG), 4-hydroxy-2-nonenal (4HNE), and nitrotyrosine and staining for granulocyte receptor-1 (Gr-1) of the neutrophils in the heart at 24 h after reperfusion were carried out (8-OHdG, 4HNE, and nitrotyrosine stainings at the Biopathology Institute, Oita, Japan; Gr-1 staining at Applied Medical Research Laboratory, Osaka, Japan) with randomized ID numbers, to ensure that the institute technicians were blind to the treatment allocation. Each harvested heart was fixed in Bouin's solution (picric acid-saturated solution:formalin:acetic acid = 15:5:1) for 3 days. Paraffin sections were prepared using a Young-type sliding microtome (Sakura Finetek Japan) with a disposable microtome blade. The sections were 4 μm thick and mounted on silane-coated slides and deparaffinized with xylene, followed by stepwise changes of the ethanol concentration.

The slides for 8-OHdG, 4HNE, and nitrotyrosine staining were treated with 1% hydrogen peroxide/methanol for 30 min to block endogenous peroxidase activity and rinsed in Tris-buffered saline. They were next treated with 8% skim milk for 30 min. Anti-8-OHdG monoclonal antibody, anti-4HNE monoclonal antibody (each diluted 1:50; Japan Institute for the Control of Aging, Nikken Seil, JaICA Japan), and anti-nitrotyrosine polyclonal antibody (diluted 1:200; 5 μg/ml diluted in PBS containing 1% BSA; Millipore) in Tris-buffered saline were applied overnight to the sections in a moisture chamber at 4°C. They were then incubated in streptavidin-biotin-peroxidase solution according to the instructions for the strept ABComplex/HRP kit (Dako Japan) for 8-OHdG and 4HNE staining or according to the instructions for the MAX-PO kit (NICHIREI, Japan) for nitrotyrosine staining. The immunoreaction was visualized by the 3,3-diaminobenzidine (DAB) reaction for 8-OHdG and 4HNE and 3-amino-9-ethylcarbazole (AEC) for nitrotyrosine. The sections were counterstained with hematoxylin.

The slides for Gr-1 were treated with 3% hydrogen peroxide for 10 min to block endogenous peroxidase activity and rinsed in distilled water and Tris-buffered saline containing Tween 20. They were next treated with blocking solution containing 0.25% casein in PBS, stabilizing protein, and 0.015 mol/l sodium azide (X0909; Dako Japan) for 5 min. Anti-mouse Gr-1 rat monoclonal antibody (diluted 1:200; MAB1037; R&D Systems, Minneapolis, MN) was applied to the sections overnight in a moisture chamber at 4°C. The slides were then incubated using the MAX-PO kit (NICHIREI, Japan) for 30 min. The immunoreaction was visualized by the DAB reaction, and the sections were counterstained with hematoxylin.

8-OHdG staining was quantified by counting the stained nuclei (brown) and all nuclei (blue and brown) in five fields (240 × 320 μm) in each section for each animal (total of 3 animals). 4HNE and nitrotyrosine stainings were quantified by the ImageJ 1.40 g software. Brown color (the color of DAB staining) for 4HNE and red color (the color of AEC staining) for nitrotyrosine were extracted in five fields (50 × 50 μm) in each section for each animal (total of 3 animals), and the stained pixel numbers were calculated. The Gr-1 staining was quantified by counting the stained cells (brown) in two fields (1.9 × 1.4 mm) in each section for each animal (total of 3 animals).

Preconditioning effect with either NO or H_2 breathing. To investigate the preconditioning effect with either NO or H_2 breathing on the infarct size, we placed anesthetized mice before the conventional 60-min occlusion of the left anterior coronary artery *1*) with no preconditioning maneuver as a control, *2*) under three times 5-min occlusion (ischemic preconditioning) in 5-min intervals, and *3*) under

three times 5-min exposure to 2% H_2 or 80 ppm NO (Fig. 7*A*). In all the procedure FIo_2 was fixed at 0.3.

Statistics. All data are presented as means + SD. A one-way ANOVA with Tukey's post hoc test was used for multiple-group comparisons for all groups. A two-way ANOVA with replication was also used for comparison among the control (antibiotics +), NO, H_2, and NO plus H_2 groups to determine the two-factor interaction between the effects of NO and H_2. Additionally, a paired *t*-test was used to compare the results of echocardiography for mice between before and after I/R.

RESULTS

Dose response curve of breathing H_2 gas concentration and infarct size. Inhalation of 1% and 2% H_2 reduced murine myocardial I/R injury size, and the effects did not significantly differ from the effect of breathing 3% H_2 (Fig. 3), as was reported in rats (10).

Inhaled NO and/or H_2 decreased the infarct size after I/R injury. The ratio of AAR to LV did not differ among groups (data not shown). The infarct size/AAR was significantly higher in mice administered antibiotics. Breathing NO, H_2, or NO plus H_2 significantly decreased the infarct size/AAR. Furthermore, the infarct size/AAR in the mice that inhaled NO plus H_2 was significantly lower than that in those that inhaled NO alone (Fig. 4, *A* and *B*), whereas the antibiotics intramuscular injection just before the I/R experiments did not show worsening in the infarct size (Fig. 4*C*), with the same AAR-to-LV ratio (data not shown), indicating no direct protective effect of antibiotics on the cardiac I/R injury. The interaction between NO and H_2 was significant ($P = 0.0052$).

The effects of the inhaled gases on the LVEF. Movement of the cardiac anterior wall of control mice was reduced after I/R, but that of mice inhaling NO plus H_2 remained unchanged (Fig. 4, *D* and *E*). The LVEF after I/R in mice breathing NO plus H_2 was significantly improved as compared with that of control mice (Fig. 4*E*). The interaction between NO and H_2 was not significant ($P = 0.4467$).

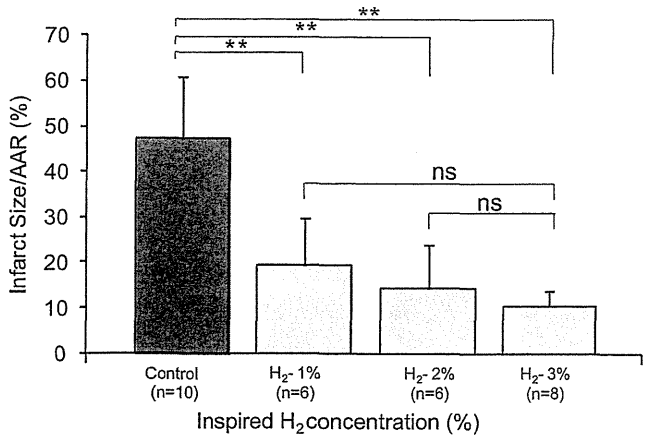

Fig. 3. Dose response curve of breathing H_2 gas concentration and infarct size. The dose dependency of inhaled H_2 on infarct size in reference to the area at risk (AAR) showed that inhalation of 1% and 2% H_2 reduced murine myocardial ischemia-reperfusion (I/R) injury size and that the effects did not significantly [not significant (ns)] differ from the effect of breathing 3% H_2. $^{**}P < 0.01$, Tukey test.

Immunohistochemical staining with antibodies against 8-OHdG. In Fig. 5, *A* and *B*, the number of nuclei, calculated as a percentage of the total number of nuclei, that showed positive staining for 8-OHdG was significantly decreased in mice that breathed NO, H_2, or NO plus H_2 as compared with that in the control mice. The number of positively stained nuclei in the mice that inhaled H_2 was significantly less than the value in mice that inhaled NO alone, but was not significantly different in mice inhaling NO plus H_2. The interaction between NO and H_2 was significant ($P < 0.0001$).

Immunohistochemical staining with antibodies against 4HNE. Intense staining of the entire area for 4HNE was observed in the control groups (Fig. 5*C*). In the NO inhalation group, the stained area was reduced, and no staining was observed in the H_2 inhalation group or the NO plus H_2 inhalation group (Fig. 5, *D* and *E*). The interaction between NO and H_2 was significant ($P = 0.0006$).

Nitrotyrosine formation in the heart tissue. The nitrotyrosine-stained area expressed as a percentage of the total area in the region of interest was large in the control (both antibiotics - and +) groups and prominent in the NO inhalation group, whereas in the mice breathing NO plus H_2 the nitrotyrosine staining was absent (Fig. 6, *A–C*). The interaction between NO and H_2 was significant ($P < 0.0001$).

Neutrophil infiltration in the heart tissue. The number of neutrophils in the region of interest in the slice was significantly decreased in the mice that inhaled NO or NO plus H_2 as compared with that in the control animals (+) (Fig. 6, *D* and *E*). The interaction between NO and H_2 was significant ($P = 0.0225$).

Preconditioning effect with either NO or H_2 breathing. As was observed and reported as the ischemic preconditioning effect before myocardial I/R, preconditioning with NO breathing before the 60-min occlusion also had effects in decreasing the infarct size, whereas H_2 breathing did not decrease the infarct size (Fig. 7*B*).

DISCUSSION

The new findings after murine myocardial I/R in this study include *1*) enterobacterial flora-derived H_2 slightly but significantly reduced myocardial infarct size; *2*) NO plus H_2 breathing completely prevented the reduction of LVEF after I/R; *3*) either NO or H_2 breathing alone decreased infarct size. The reduction of infarct size was significantly greater in mice that inhaled NO plus H_2 than in those breathing NO alone; *4*) staining for reactive oxygen species (ROS) markers and neutrophils was reduced after NO and/or H_2 inhalation; *5*) NO inhalation enlarged the myocardial staining area for nitrotyrosine, whereas H_2 inhalation completely eliminated the staining for nitrotyrosine; *6*) preconditioning with NO before I/R decreased the infarct area, whereas preconditioning with H_2 did not.; and *7*) repetitive two-way ANOVA revealed a significant interaction between the effects of NO and H_2 on the infarct size, ROS and nitrotyrosine production, and neutrophil infiltration.

The finding that the presence of enterobacterial flora caused a slight but significant reduction in infarct size suggests loss of H_2-producing enterobacteria is a risk factor for massive infarction after I/R in the heart, and possibly in the brain, and may be clinically significant. It has also been reported in humans that the composition of the gut flora varies among individuals (21)

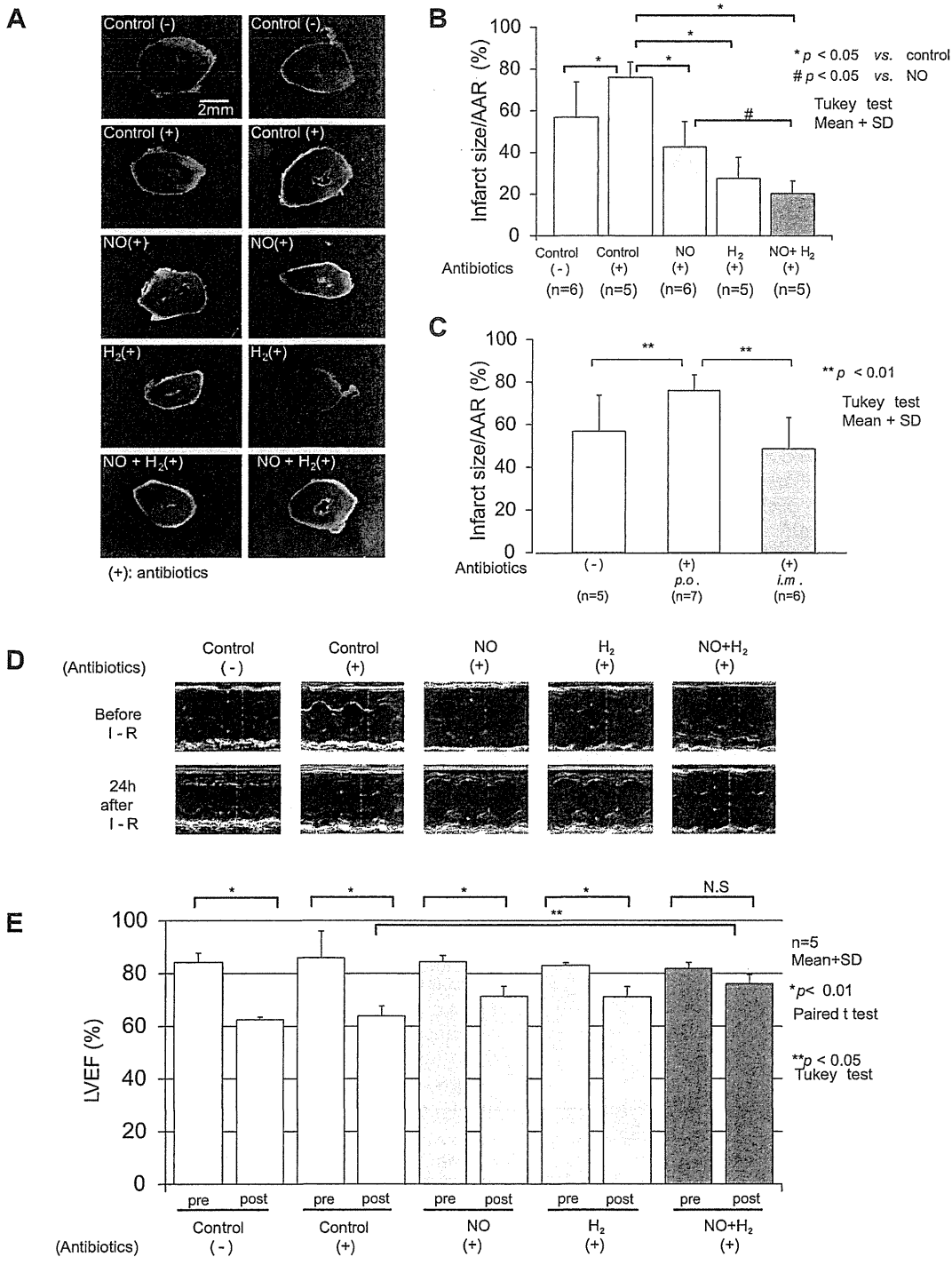

Fig. 4. Effects of the inhaled gas species on infarct size and heart function. *A*: representative cross sections after triphenyltetrazolium chloride staining in each group. *B*: ratio of infarct size to AAR (infarct size/AAR) was significantly larger in mice given antibiotics. Breathing NO, H_2, and NO plus H_2 significantly decreased the infarct size/AAR. The infarct size/AAR in mice that inhaled NO plus H_2 was significantly lower than that of the mice that breathed NO only. *C*: to exclude the possible direct protective effects of antibiotics on the infarct size after I/R, the antibiotics were given per os (p.o.) as in the protocol (Fig.1) or injected intramuscularly (i.m.) just before the I/R experiments, and no worsening in the infarct size by intramuscular injection has been observed, indicating no direct effect of antibiotics on the infarct size. *D*: typical echocardiographic image at 24 h after I/R. *E*: LV ejection fraction (LVEF) of mice before and at 24 h after I/R. LVEF was significantly decreased at 24 h after I/R, except in mice that inhaled NO plus H_2. LVEF after I/R in the mice inhaling NO plus H_2 was significantly improved compared with that in the control mice. Data are presented as means + SD. NS, not significant.

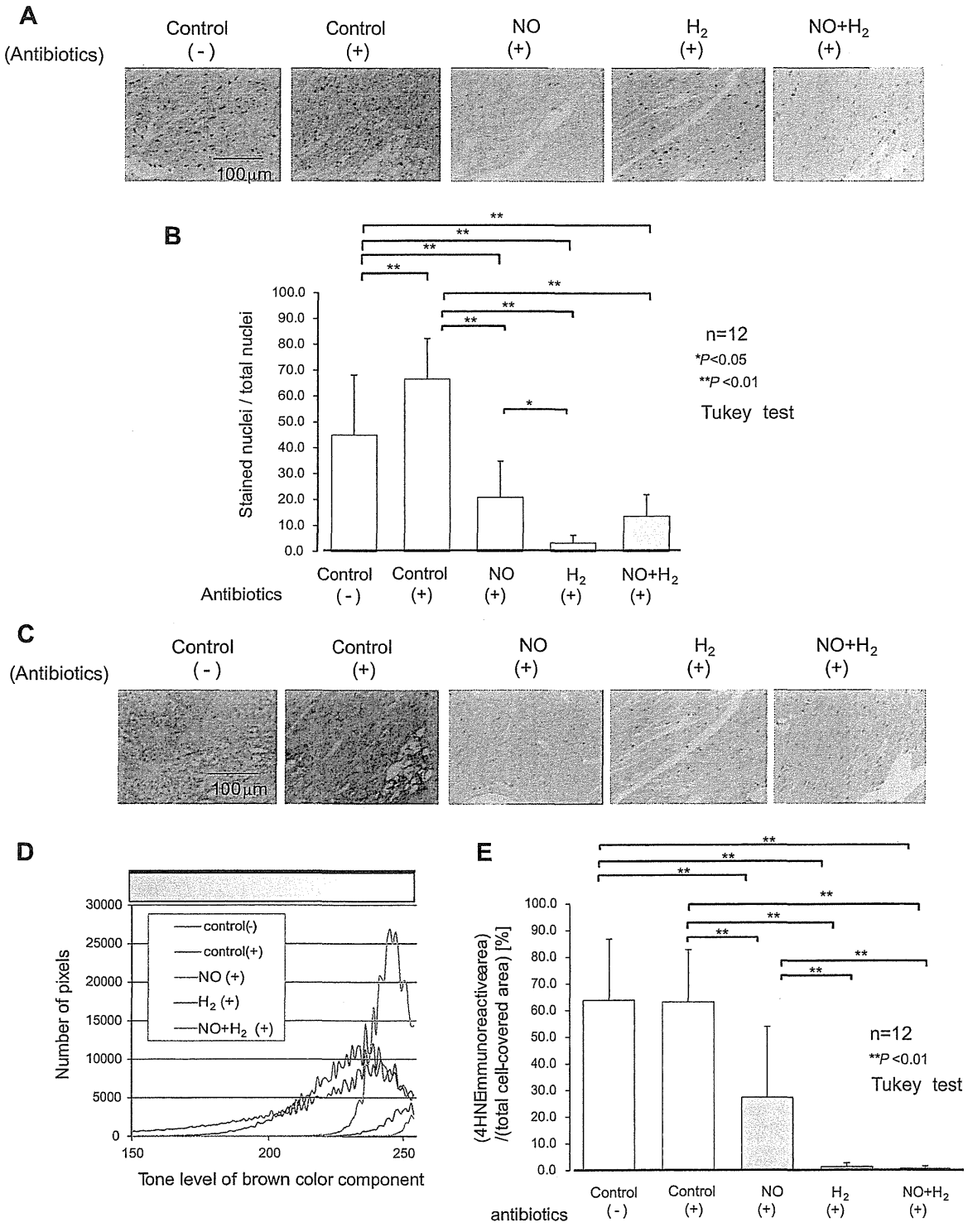

Fig. 5. Immunohistochemical staining for 8-hydroxy-2′-deoxyguanosine and 4-hydroxy-2-nonenal (4HNE). *A*: nuclei stained blue with hematoxylin and stained brown by the 3,3-diaminobenzidine (DAB) reaction using primary antibody against 8-hydroxy-2′-deoxyguanosine. *B*: number of 8-hydroxy-2′-deoxyguanosine-immunoreactive nuclei, expressed as a percentage of the total number of nuclei in the region of interest in the slice, was significantly decreased in the mice that inhaled NO, H_2, or NO plus H_2. *C*: nuclei stained blue with hematoxylin and cells stained brown by the DAB reaction using antibody against 4HNE. *D*: histogram of the brown color of each image extracted by color deconvolution. The tone level of the brown color component of each pixel was presented on a scale of 0 (brown) to 255 (white). *E*: 4HNE-immunoreactive area was expressed as a percentage of the total area in the region of interest of the slice. Intense staining for 4HNE was observed in the entire infarct area in control groups. Inhalation of NO reduced the stained area as compared with that of control group. The stained area was eliminated in both the H_2 group and the H_2 plus NO group. Data are presented as means + SD.

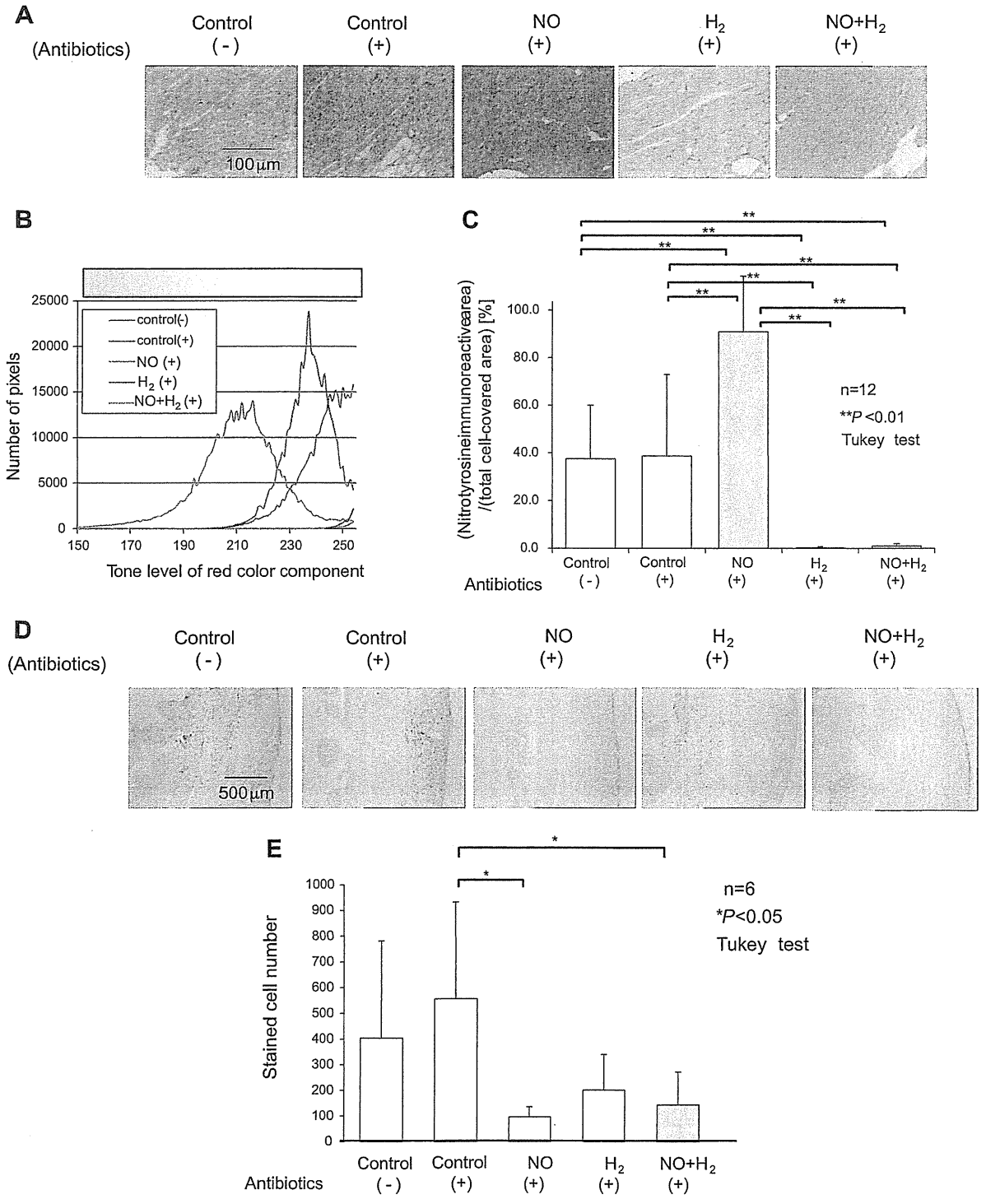

Fig. 6. Immunohistochemical staining for nitrotyrosine and neutrophils. *A*: nuclei stained blue with hematoxylin and cells stained red by the 3-amino-9-ethylcarbazole reaction using antibody against with nitrotyrosine. *B*: histogram of the red color regions of each image extracted by color deconvolution. The tone level of the red color component of each pixel was presented on a scale of 0 (red) to 255 (white). *C*: nitrotyrosine-immunoreactive area (number of pixels of red color) was expressed as a percentage of the total area covered by the cells (number of pixels covered by the cells) in each section. The nitrotyrosine-immunoreactive area was significantly larger in the NO group than in other groups. Nitrotyrosine immunostaining was completely absent in both the H_2 group and NO plus H_2 groups. *D*: neutrophils stained brown by the DAB reaction after incubation with a primary antibody against granulocyte receptor-1, and the nuclei stained blue with hematoxylin. *E*: number of neutrophils in the region of interest in the slice was significantly decreased in the mice that inhaled NO or NO plus H_2 as compared with that in the control animals (+). Data are presented as means + SD.

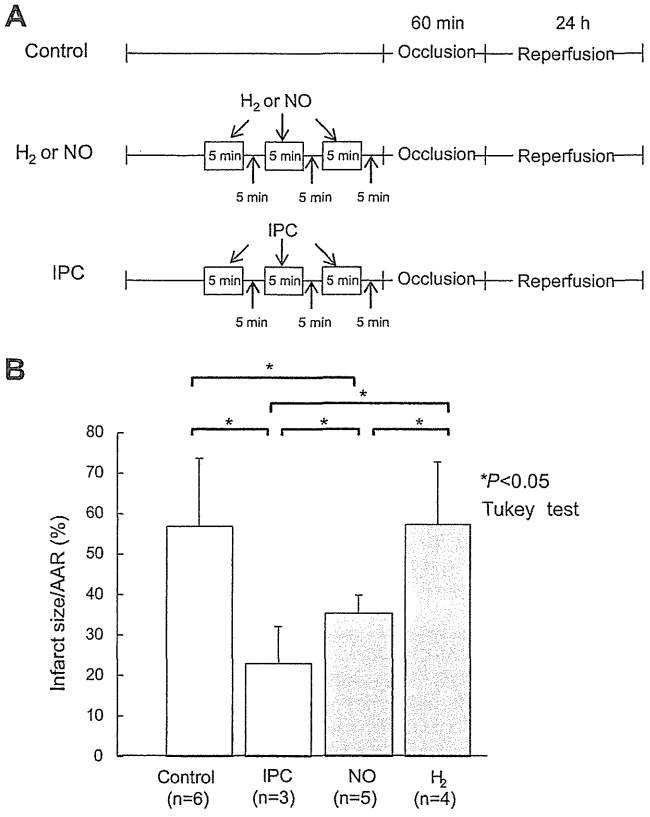

Fig. 7. Preconditioning effect with either NO or H_2 breathing. *A*: ischemic preconditioning (IPC) effect as well as preconditioning effect with NO or H_2 breathing on infarction size after I/R injury was investigated. The coronary artery was occluded or mice breathed NO or H_2 for 5 min in 5-min intervals 3 times before the conventional 60-min occlusion of the left anterior coronary artery. *B*: preconditioning with NO breathing before the 60-min occlusion also had effects in decreasing the infarct size, whereas preconditioning with H_2 breathing did not decrease the infarct size.

from H_2-dominant production to methane dominant. A number of probiotic supplements are reported to be cardioprotective, while their effect may not be related to H_2 production; on the other hand, the cardioprotective effect of dietary fiber (23) may be related to H_2 production. Poorly digestible fiber debris is transported to the distal intestine, where anaerobes ferment the debris, and produce not only H_2, but also methane, hydrogen sulfide, and so on. Therefore, it cannot be excluded that antibiotics also eliminated other potential cardioprotective gases. It would be interesting to study the specific protective effect of H_2 by inoculating wild-type bacteria producing H_2 and gene-manipulated bacteria unable to produce H_2 after clearing the enteric bacteria, similar to the strategy used for demonstrating the protective role of H_2-producing *Escherichia coli* against Concanavalin A-induced hepatitis (11).

Although the persistent but low-dose production of H_2 by enteric bacteria may contribute to reduction in the infarct size, or the dose-response relation for H_2 on the infarct size may be very steep, it should be noted that enterobacterial flora-derived gases were not sufficiently potent for cardioprotection after I/R injury, since inhalation of H_2 even in the presence of enterobacterial flora significantly reduced the infarct size (Fig. 3).

Nagasaka et al. (18) have shown that the cardioprotective effects of inhaled NO require the presence of soluble guanylate cyclase-α_1, and the results of their study suggested that bone marrow-derived cells are mediators of the ability of NO to attenuate cardiac I/R injury. Therefore, it is possible that a primary role of NO is to inhibit recruitment of leukocytes from blood stream to the heart. Their finding of the local effect of NO during myocardical I/R injury is in line with our finding of reduced neutrophil infiltration observed following NO inhalation, as well as of the in vivo preconditioning cardioprotective effect of NO breathing before the induction of I/R injury on the infarct size.

Ohsawa et al. (19) showed in an in vitro study that H_2 gas can reduce hydroxyl radicals. However, the reaction of H_2 with hydroxyl radicals is controversial. Because the half-life of hydroxyl radicals is short, 10^{-9} s (24), Wood and Gladwin (29) noted that the hydroxyl radical is too short-lived to react with H_2, and will react with several cellular components before reacting with less abundant H_2 molecules. As compared with that of hydroxyl radicals, the half-life of peroxynitrite is long, 0.05–1 s (24), and peroxynitrite has a greater chance to react with H_2 in areas of I/R injury. H_2 molecules are very diffusible and may reach ischemic tissues even before reperfusion (10). During I/R, they will eliminate peroxynitrite (and possibly hydroxyl radicals), thereby suppressing inflammation and cellular apoptosis. Concerning the mechanism of the effects of H_2 gas, other possible sites of action of H_2 have been suggested, such as induction of hemoxygenase 1 (4) and heat shock protein (28). These possibilities need to be further investigated.

A comparison of the effects of inhaled NO with those of inhaled H_2 in our study revealed that they exerted equivalent cardioprotective effect, both in terms of improving the cardiac function and reducing the infarct size. The ROS markers, 8-OHdG and 4HNE, were similarly eliminated. A major difference between the effects of NO and H_2 breathing is the production of nitrotyrosine in the tissue affected by I/R injury in NO breathing. The increased amount of nitrotyrosine produced by inhaled NO suggests that some adverse effects on signal trafficking and cellular function may occur sooner or later by the RNS reactions with the tyrosine at the active site of vital enzymes and cellular components.

It should be noted that we used the maximal concentration of NO, 80 ppm, as had been reported to be effective in the protection of heart against I/R injury. Furthermore, we placed the mice under the minimal contribution of enterobacterial flora-derived H_2 by administrating antibiotics with fasting. It is possible that less NO inhalation with more enterobacterial flora-derived H_2 might potently protect the heart from I/R injury, but even in that case H_2 inhalation would minimize the potential risk caused by nitrotyrosine production.

Other potential methods to reduce peroxynitrite production while maintaining the beneficial effects of inhaled NO could be to use a peroxynitrite decomposition catalyst (14, 27) or increase the cGMP concentration in the cells by using a soluble guanylyl cyclase activator (22) or phosphodiesterase-5 inhibitor (16), since these enhancers of NO effects via cGMP induction may enable reduction of the inhaled NO concentration, thereby decreasing peroxynitrite formation and minimizing the adverse effects of NO inhalation.

One of the limitations of this in vivo study was that young male mice were used for this study, whereas myocardial I/R

injury typically occurs in older individuals with comorbid risk factors such as diabetes and atherosclerosis; furthermore, many cardioprotective interventions that are effective in younger animals are not effective in older animals or in the presence of risk factors, a phenomenon that may be related to chronic oxidative stress (31). Therefore, it will be important to verify our study findings in older mice and in relation to enterobacterial flora-derived H_2.

In conclusion, inhaled NO suppresses the inflammation in I/R tissues and H_2 eliminates the adverse by-products of NO exposure, peroxynitrite. Thus our study supports the view that NO and H_2 are suggestive partners that can be used as a mixture for breathing during coronary interventions.

ACKNOWLEDGMENTS

We thank Dr. Warren M. Zapol (Department of Anesthesia and Critical Care, Massachusetts General Hospital, Harvard Medical School) for his critique of our manuscript and Masumi Tanaka (Department of Respiratory Medicine, Kitasato Univ.) for excellent technical assistance.

GRANTS

This work was supported by Grant-in-Aid No. 21591002 from the Ministry of Education, Culture, Sports, Science and Technology, Japan (to H. Kobayashi) and a Kitasato University Grant for International Exchange Programs for 2009–2012 (to H. Kobayashi and K. Kokubo).

DISCLOSURES

No conflicts of interest, financial or otherwise, are declared by the author(s).

AUTHOR CONTRIBUTIONS

Author contributions: T.S., Y.S., S.H., and R.H. performed experiments; T.S. and K.K. analyzed data; T.S., K.K., Y.S., S.H., R.H., M.H., and H.K. approved final version of manuscript; K.K. prepared figures; K.K. and H.K. edited and revised manuscript; R.H., M.H., and H.K. conception and design of research; R.H., M.H., and H.K. interpreted results of experiments; H.K. drafted manuscript.

REFERENCES

1. **American Institute of Aeronautics and Astronautics.** *Guide to Safety of Hydrogen, and Hydrogen Systems.* Virginia, 2005.
2. **Brown GC, Borutaite V.** Nitric oxide and mitochondrial respiration in the heart. *Cardiovasc Res* 75: 283–290, 2007.
3. **Brüne B, Lapetina EG.** Activation of a cytosolic ADP-ribosyltransferase by nitric oxide-generating agents. *J Biol Chem* 264: 8455–8458, 1989.
4. **Buchholz BM, Masutani K, Kawamura T, Peng X, Toyoda Y, Billiar TR, Bauer AJ, Nakao A.** Hydrogen-enriched preservation protects the isogeneic intestinal graft and amends recipient gastric function during transplantation. *Transplantation* 92: 985–992, 2011.
5. **Calabrese V, Cornelius C, Rizzarelli E, Owen JB, Dinkova-Kostova AT, Butterfield DA.** Nitric oxide in cell survival: a janus molecule. *Antioxid Redox Signal* 11: 2717–2739, 2009.
6. **Fox-Robichaud A, Payne D, Hasan SU, Ostrovsky L, Fairhead T, Reinhardt P, Kubes P.** Inhaled NO as a viable antiadhesive therapy for ischemia/reperfusion injury of distal microvascular beds. *J Clin Invest* 101: 2497–2505, 1998.
7. **Fukuda K, Asoh S, Ishikawa M, Yamamoto Y, Ohsawa I, Ohta S.** Inhalation of hydrogen gas suppresses hepatic injury caused by ischemia/reperfusion through reducing oxidative stress. *Biochem Biophys Res Commun* 361: 670–674, 2007.
8. **Guery B, Neviere R, Viget N, Foucher C, Fialdes P, Wattel F, Beaucaire G.** Inhaled NO preadministration modulates local and remote ischemia-reperfusion organ injury in a rat model. *J Appl Physiol* 87: 47–53, 1999.
9. **Hataishi R, Rodrigues AC, Neilan TG, Morgan JG, Buys E, Shiva S, Tambouret R, Jassal DS, Raher MJ, Furutani E, Ichinose F, Gladwin MT, Rosenzweig A, Zapol WM, Picard MH, Bloch KD, Scherrer-Crosbie M.** Inhaled nitric oxide decreases infarction size and improves left ventricular function in a murine model of myocardial ischemia-reperfusion injury. *Am J Physiol Heart Circ Physiol* 291: H379–H384, 2006.
10. **Hayashida K, Sano M, Ohsawa I, Shinmura K, Tamaki K, Kimura K, Endo J, Katayama T, Kawamura A, Kohsaka S, Makino S, Ohta S, Ogawa S, Fukuda K.** Inhalation of hydrogen gas reduces infarct size in the rat model of myocardial ischemia-reperfusion injury. *Biochem Biophys Res Commun* 373: 30–35, 2008.
11. **Kajiya M, Sato K, Silva MJ, Ouhara K, Do PM, Shanmugam KT, Kawai T.** Hydrogen from intestinal bacteria is protective for Concanavalin A-induced hepatitis. *Biochem Biophys Res Commun* 386: 316–321, 2009.
12. **Kinobe R, Ji Y, Nakatsu K.** Peroxynitrite-mediated inactivation of heme oxygenases. *BMC Pharmacol* 4: 26, 2004.
13. **Liu X, Huang Y, Pokreisz P, Vermeersch P, Marsboom G, Swinnen M, Verbeken E, Santos J, Pellens M, Gillijns H, Van de Werf F, Bloch KD, Janssens S.** Nitric oxide inhalation improves microvascular flow and decreases infarction size after myocardial ischemia and reperfusion. *J Am Coll Cardiol* 50: 808–817, 2007.
14. **Maybauer DM, Maybauer MO, Szabó C, Cox RA, Westphal M, Kiss L, Horvath EM, Traber LD, Hawkins HK, Salzman AL, Southan GJ, Herndon DN, Traber DL.** The peroxynitrite catalyst WW-85 improves pulmonary function in ovine septic shock. *Shock* 35: 148–155, 2011.
15. **McMahon TJ, Doctor A.** Extrapulmonary effects of inhaled nitric oxide: role of reversible S-nitrosylation of erythrocytic hemoglobin. *Proc Am Thorac Soc* 3: 153–160, 2006.
16. **Merkus D, Visser M, Houweling B, Zhou Z, Nelson J, Duncker DJ.** Phosphodiesterase 5 inhibition-induced coronary vasodilation is reduced after myocardial infarction. *Am J Physiol Heart Circ Physiol* 304: H1370–H1381, 2013.
17. **Moncada S, Higgs EA.** Nitric oxide and the vascular endothelium. *Handb Exp Pharmacol*: 213–254, 2006.
18. **Nagasaka Y, Buys ES, Spagnolli E, Steinbicker AU, Hayton SR, Rauwerdink KM, Brouckaert P, Zapol WM, Bloch KD.** Soluble guanylate cyclase-α_1 is required for the cardioprotective effects of inhaled nitric oxide. *Am J Physiol Heart Circ Physiol* 300: H1477–H1483, 2011.
19. **Ohsawa I, Ishikawa M, Takahashi K, Watanabe M, Nishimaki K, Yamagata K, Katsura K, Katayama Y, Asoh S, Ohta S.** Hydrogen acts as a therapeutic antioxidant by selectively reducing cytotoxic oxygen radicals. *Nat Med* 13: 688–694, 2007.
20. **Radi R.** Nitric oxide, oxidants, and protein tyrosine nitration. *Proc Natl Acad Sci USA* 101: 4003–4008, 2004.
21. **Rumessen JJ.** Hydrogen and methane breath tests for evaluation of resistant carbohydrates. *Eur J Clin Nutr* 46, *Suppl* 2: S77–S90, 1992.
22. **Salloum FN, Das A, Samidurai A, Hoke NN, Chau VQ, Ockaili RA, Stasch JP, Kukreja RC.** Cinaciguat, a novel activator of soluble guanylate cyclase, protects against ischemia/reperfusion injury: role of hydrogen sulfide. *Am J Physiol Heart Circ Physiol* 302: H1347–H1354, 2012.
23. **Satija A, Hu FB.** Cardiovascular benefits of dietary fiber. *Curr Atheroscler Rep* 14: 505–514, 2012.
24. **Sies H.** Strategies of antioxidant defense. *Eur J Biochem* 215: 213–219, 1993.
25. **Snyder SH.** Janus faces of nitric oxide. *Nature* 364: 577, 1993.
26. **Suematsu M, Suganuma K, Kashiwagi S.** Mechanistic probing of gaseous signal transduction in microcirculation. *Antioxid Redox Signal* 5: 485–492, 2003.
27. **Szabó C, Mabley JG, Moeller SM, Shimanovich R, Pacher P, Virag L, Soriano FG, Van Duzer JH, Williams W, Salzman AL, Groves JT.** Part I: pathogenetic role of peroxynitrite in the development of diabetes and diabetic vascular complications: studies with FP15, a novel potent peroxynitrite decomposition catalyst. *Mol Med* 8: 571–580, 2002.
28. **Tanaka Y, Shigemura N, Kawamura T, Noda K, Isse K, Stolz DB, Billiar TR, Toyoda Y, Bermudez CA, Lyons-Weiler J, Nakao A.** Profiling molecular changes induced by hydrogen treatment of lung allografts prior to procurement. *Biochem Biophys Res Commun* 425: 873–879, 2012.
29. **Wood KC, Gladwin MT.** The hydrogen highway to reperfusion therapy. *Nat Med* 13: 673–674, 2007.
30. **Yoshida A, Asanuma H, Sasaki H, Sanada S, Yamazaki S, Asano Y, Shinozaki Y, Mori H, Shimouchi A, Sano M, Asakura M, Minamino T, Takashima S, Sugimachi M, Mochizuki N, Kitakaze M.** H_2 Mediates cardioprotection via involvements of K^{ATP} channels and permeability transition pores of mitochondria in dogs. *Cardiovasc Drugs Ther* 26: 217–226, 2012.
31. **Zhu J, Rebecchi MJ, Wang Q, Glass PS, Brink PR, Liu L.** Chronic Tempol treatment restores pharmacological preconditioning in the senescent rat heart. *Am J Physiol Heart Circ Physiol* 304: H649–H659, 2013.

J Artif Organs (2013) 16:193–205
DOI 10.1007/s10047-013-0686-4

ORIGINAL ARTICLE

Activation of platelets upon contact with a vitamin E-coated/non-coated surface

Hiroshi Tsukao · Kenichi Kokubo · Haruko Takahashi · Mina Nagasato · Takanori Endo · Naoto Iizuka · Toshihiro Shinbo · Minoru Hirose · Hirosuke Kobayashi

Received: 23 May 2012 / Accepted: 11 January 2013 / Published online: 5 February 2013

Abstract The purpose of this study was to determine the effects of a vitamin E-coated surface on platelet activation, focusing on the interactions among the vitamin E-coated surface, platelets and leukocytes. Platelet-rich plasma (PRP) or PRP containing leukocytes (LPRP) was used. No difference was observed in platelet activation between PRP and LPRP for a vitamin E-coated membrane, meaning that platelet activation triggered by leukocytes was suppressed in plasma coming in contact with a vitamin E-coated membrane, while the membrane itself directly induced platelet activation. The antioxidant capacity of the vitamin E-coated membrane in contact with PRP or LPRP was partially reduced, but sufficient residual capacity remained. The in vitro experiments using an oxidized vitamin E-coated surface revealed that P-selectin expression and superoxide anion production in the platelets and platelet adhesion were induced by contact with the oxidized vitamin E-coated surface. We conclude that contact with a vitamin E-coated surface reduces platelet activation mediated by superoxide anions, probably by reducing superoxide anions, but during the process of the reduction, the vitamin E-coated surface itself becomes oxidized, which again causes platelet activation. The beneficial effects of a vitamin E-coated dialyzer in respect of platelet activation were counteracted by the formation of oxidized vitamin E.

Keywords Leukocyte activation · Platelet activation · Superoxide anion · Vitamin E-coated surface · Hemodialysis

Abbreviations

APF	Aminophenyl fluorescein
EDTA	Ethylenediaminetetraacetate
fMLP	*N*-formyl-methionyl-leucyl-phenylalanine
FRAP assay	Ferric-reducing antioxidant power assay
LPRP	PRP with leukocytes
NO	Nitric oxide
PBS	Phosphate-buffered saline
PRP	Platelet-rich plasma
ROS	Reactive oxygen species
SOD	Superoxide dismutase
TPTZ	2,4,6-Tripyridyl-s-triazine
WST-1	2-(4-Iodophenyl)-3-(4-nitrophenyl)-5-(2,4-disulfophenyl)-2H-tetrazolium monosodium salt
XOD	Xanthine–xanthine oxidase

Introduction

Vascular diseases, including arteriosclerosis and coronary artery disease, often show progression in patients undergoing

H. Tsukao · K. Kokubo · M. Hirose · H. Kobayashi
Kitasato University Graduate School of Medical Sciences, Kanagawa, Japan

H. Tsukao
Department of Clinical Engineering, School of Health Science, Tokyo University of Technology, Tokyo, Japan

K. Kokubo (✉) · H. Kobayashi (✉)
Department of Medical Engineering and Technology, School of Allied Health Sciences, Kitasato University, 1-15-1 Kitasato, Sagamihara, Minami-ku, Kanagawa 252-0373, Japan
e-mail: kokubo@kitasato-u.ac.jp

H. Kobayashi
e-mail: hiro@kitasato-u.ac.jp

K. Kokubo · H. Takahashi · M. Nagasato · T. Endo · N. Iizuka · T. Shinbo · M. Hirose · H. Kobayashi
Kitasato University School of Allied Health Sciences, Kanagawa, Japan

hemodialysis [1, 2]. Increased oxidative stress [3] and platelet reactivity [4, 5] are considered to be the major factors underlying the initiation and progression of these diseases. High plasma levels of oxidative stress markers, including oxidized protein products and peroxidized lipids, are observed in patients on maintenance hemodialysis [6–8]. Peroxidized low-density lipoprotein affects the functions of endothelial cells and granulocytes, thereby increasing their potential to initiate and accelerate the progression of atherosclerosis [9–14]. Platelet reactivity, which is also increased in patients undergoing hemodialysis [15], has been reported to be positively correlated with the incidence of coronary artery disease [4, 16, 17].

Vitamin E acts as a powerful scavenger protecting plasma lipids and the cell membrane from oxidative events [18] and also acts as an inhibitor of platelet aggregation and adhesion [19–23]. Vitamin E-coated dialysis membranes were developed with the aim of providing antioxidant protection, as well as increasing the biocompatibility of the dialysis membrane [24]. Clinical studies have confirmed that the use of vitamin E-coated membranes is associated with reduced plasma levels of oxidative stress-related markers [25–29].

However, the beneficial effects of vitamin E coating of dialysis membranes on platelet activation have not yet been clearly demonstrated in the clinical setting [27]. Use of vitamin E-coated membranes has been shown to be associated with reduced levels of oxidative stress markers in patients, but it has not been shown to alter platelet activation, as evaluated by soluble P-selectin, despite the fact that vitamin E itself has been demonstrated to inhibit platelet activation and adhesion [19–23]. The reason why vitamin E-coating did not suppress platelet activation in the clinical setting remains to be elucidated.

Previous studies have demonstrated that there are mutual interactions, or "cross talk," between platelets and leukocytes. Platelets influence leukocyte activation [30, 31]. For instance, platelet-released substances, such as adenine nucleotides, platelet-derived growth factor, platelet factor 4 and thromboxane A2, are reported to induce leukocyte activation or promote superoxide anion generation by neutrophils [31]. Platelets bound to neutrophils [32–34] are also known to promote the generation of superoxide anions by neutrophils. By contrast, superoxide anion generation and cytotoxicity of neutrophils have been reported to be inhibited by unstimulated platelets, and leukocyte chemotaxis and adhesion are known to be inhibited by platelet-released nitric oxide (NO) [35] and soluble P-selectin [36]. Leukocytes also influence platelet activation [30, 31]. Leukocytes and leukocyte-released superoxide anions have been reported to enhance platelet adhesion [37]. Furthermore, leukocyte-released substances, such as superoxide anions, platelet-activating factor, elastase and cathepsin G, have been reported to induce platelet aggregation [37]. Conversely, unstimulated or weakly activated leukocytes have also been reported to attenuate platelet aggregation, probably via leukocyte-released NO [38] and/or ADPase [39]. Since superoxide anions are one of the important mediators of the interactions between leukocytes and platelets, it was considered that use of vitamin E-coated membranes could reduce the mutual activation of these cells during hemodialysis treatments. Therefore, to clarify the effects of vitamin E-coating on the platelets during hemodialysis, we considered that is important to conduct investigations in the context of the interactions among the vitamin E-coated surface, platelets and leukocytes.

The antioxidant actions of vitamin E have been ascribed to the hydrogen abstraction reaction from the phenolic hydroxyl group [40–43]. However, when vitamin E coated onto a dialysis membrane acts as an antioxidant, the vitamin E itself becomes oxidized, resulting in the generation of oxidized products of vitamin E, such as α-tocopherylquinone, hydroperoxytocopherone, etc. [44]. Therefore, when reducing agents such as ascorbic acid, which can regenerate vitamin E from vitamin E radicals, are not abundant in the blood of patients undergoing dialysis, the oxidized vitamin E remains oxidized and increases in amount with the progress of hemodialysis, potentially causing platelet activation. However, the effects of oxidized vitamin E on platelet activation have not yet been examined in detail.

Considering these possible influences of vitamin E-coated dialysis membranes on platelets, we hypothesized that the platelet activation in plasma coming in contact with a vitamin E-coated membrane may be related to the oxidation of vitamin E on the surface. The purpose of this study was to clarify the interactions among the vitamin E-coated surface, platelets and leukocytes in respect to vitamin E oxidation. As a result, the oxidized vitamin E-coated surface was found to induce platelet activation, which could be a reason why the beneficial effect of vitamin E on platelet activation could not be clearly appreciated in the clinical setting even though the other oxidative stress markers were reduced by the use of vitamin E-coated membranes.

Materials and methods

Preparation of platelet-rich plasma

Fresh porcine blood was obtained from a dealer in animal blood and organs for research use (Tokyo Shibaura Zoki, Tokyo, Japan) on the morning of the day of the experiments. Sodium citrate was added to the blood (final

concentration 10 mM), and the blood was carefully transferred to our laboratory in a cooling box. Two kinds of solutions were prepared: platelet-rich plasma (PRP), which was prepared as a supernatant solution separated from porcine whole blood by centrifugation at 140 g for 20 min, and platelet-rich plasma with leukocytes (LPRP), prepared by adding a leukocyte interface layer formed on the sedimented erythrocyte layer when whole blood was centrifuged to obtain PRP as the supernatant. The leukocyte interface layer added to the PRP was approximately 80 ml in volume when 250 ml of whole blood was centrifuged. Platelet and leukocyte counts were adjusted to the original cell composition of the blood.

Sample preparation for determining the effects of superoxide stimulation on platelet activation

This experiment was performed in vitro without allowing any contact of the plasma with the dialysis membrane to confirm that the platelet and leukocyte interactions were mediated by superoxide anions in LPRP prepared from porcine whole blood. PRP or LPRP prepared from the blood of one animal was divided into six portions. Changes in the percentage of activated platelets were measured after the addition of xanthine–xanthine oxidase (XOD) or *N*-formyl-methionyl-leucyl-phenylalanine (fMLP) to the PRP or LPRP. We also checked whether superoxide dismutase (SOD) suppressed the platelet activation induced by activated leukocytes. The prepared samples for measuring superoxide anions and P-selectin expression were: control, with SOD, with XOD, with XOD + SOD, with fMLP and with fMLP + SOD (Tables 1, 2). SOD solution was prepared by diluting SOD (Wako Pure Chemical Industries Ltd., Osaka, Japan) using the dilution buffer and adjusting the concentration to 1,000 U/ml. The fMLP solution (1 μM) was also prepared by diluting fMLP (Wako Pure Chemical Industries, Ltd.) using the same dilution buffer. The buffer solution used to dilute SOD or fMLP was one containing xanthine in the SOD Assay Kit (Dojindo Laboratories, Kumamoto, Japan). The superoxide anion concentration and expression of P-selectin on the platelet surface were measured immediately after incubation for 20 min (plus 10 min during centrifugation) and 10 min (plus 20 min during centrifugation), respectively (as described below).

Measurement of superoxide anion production

2-(4-Iodophenyl)-3-(4-nitrophenyl)-5-(2,4-disulfophenyl)-2H-tetrazolium monosodium salt (WST-1 in the SOD assay kit, Dojindo Laboratories), which produces a water-soluble formazan dye upon reduction with superoxide anions, was used to detect superoxide anions. The reduction rate of superoxide anions detected by formazan dye has been reported to be linearly related to the xanthine oxidase activity and to be inhibited by SOD [45]. We determined the concentrations of the superoxide anions based on the absorbance of the formazan dye.

Collected samples with or without SOD, XOD, fMLP or dilution buffer (total volume 60 μl) were placed in the wells of a 96-well microplate, followed by the addition of 200 μl of WST working solution, comprising diluted WST-1 (1/20 dilution using the buffer solution containing xanthine supplied by the manufacturer). Wells without samples, to which 60 μl of dilution buffer and 200 μl of WST working solution were added, were used as blank wells for the baseline measurements. We also prepared samples to which 20 μl of 1,000 U/ml of SOD (WK-013, Funakoshi Corp., Tokyo, Japan) was added to confirm whether it was actually the superoxide anions that were inducing the production of formazan dye from WST-1 and activated platelets. After incubation at 37 °C for 20 min, the samples were centrifuged at 3,000*g* for 10 min. The absorbance of the supernatant was measured using a microplate reader (model 680, Bio-Rad Laboratories, Inc., CA, USA) at a wavelength of 450 nm (reference wavelength 655 nm).

Measurement of the expression of P-selectin on the platelet surface

Platelet activation was determined by assessing the platelet surface expression of P-selectin by flow cytometry (FACS Calibur™, Becton-Dickinson & Co., Franklin Lakes, NJ, USA). P-selectin expression was assessed using a

Table 1 Prepared samples for measuring superoxide anions

	Sample (μl)	XOD (μl)	SOD (μl)	fMLP (μl)	Dilution buffer (μl)
Control	20				40
SOD	20		20		20
XOD	20	20			20
XOD + SOD	20	20	20		
fMLP	20			20	20
fMLP + SOD	20		20	20	

Table 2 Prepared samples for measuring P-selectin

	Sample (μl)	XOD (μl)	SOD (μl)	fMLP (μl)	Dilution buffer (μl)
Control	200				200
SOD	200		100		100
XOD	200	100			100
XOD + SOD	200	100	100		
fMLP	200			100	100
fMLP + SOD	200		100	100	

phycoerythrin-conjugated anti-CD62P antibody (0.3 mg/ml, BioCytex, Marseille, France), a mouse monoclonal antibody against human P-selectin. Prior to the analysis, we confirmed that the antibody cross-reacted with porcine P-selectin on platelets activated with bovine thrombin (Wako Pure Chemical Industries Ltd., Osaka, Japan).

After the PRP or LPRP was incubated with SOD, XOD, fMLP for 10 min, the solution was transferred into a sterile tube and was centrifuged at 3,000 rpm for 20 min. After the supernatant solution had been removed, 400 μl of EDTA-PBS (containing 9 mM of ethylenediaminetetraacetate in 0.2 M, pH 7.4, of phosphate-buffered saline) was added to the pellet to wash the platelets, followed by centrifugation at 7,600 rpm (4,000*g*) for 1 min. After washing the platelets twice with EDTA-PBS and once with PBS, the platelets were suspended in 400 μl of PBS. The antibody solution (20 μl) was added and vortexed, followed by incubation for 45 min at room temperature. After incubation, 400 μl of 1 % PBS-buffered paraformaldehyde was added and vortexed, followed by incubation for 7 min for fixation. The treated platelets were washed with 600 μl of PBS and centrifuged at 7,600 rpm for 1 min. The procedure was repeated twice, then 1 ml of PBS was added to the pellet to prepare a platelet suspension. The platelet suspensions were analyzed by flow cytometry, and platelets were identified based on the particle size (forward scatter) and complexity (side scatter). Light scatter and fluorescence data from 10,000 platelet events were collected with all detectors in a logarithmic mode. Acquisition and processing data were analyzed using BD Cell Quest, ver. 3.3 (Becton, Dickinson & Co.). Platelet activation was expressed as the percentage of platelets that were positive for antibody binding.

Circulation of PRP and LPRP in hollow-fiber dialysis membranes

A vitamin E-coated polysulfone membrane, VPS-13H®, and a non-coated polysulfone membrane, APS-15MD®, (Asahi Kasei Kuraray Medical, Tokyo, Japan) were used (Table 3) to examine the effects on the activation of platelets when the plasma was placed in contact with the dialysis membrane. A circulating circuit was prepared with a dialyzer and blood circuit connecting both the blood inlet and outlet to a soft bag (FCB-3, Asahi Kasei Kuraray Medical, Tokyo, Japan). After priming both the blood side and dialysate side with saline, 500 ml of saline solution was left on the blood side of the circuit connected with the dialyzer and soft bag, and then 500 U of heparin sodium (Fuso Pharmaceutical Industries, Ltd., Osaka, Japan), which is the most frequently used anticoagulant during hemodialysis, were added. Then 500 ml of PRP or LPRP was added to the bag. The final concentration of heparin was 500 U/l. The PRP or LPRP diluted with heparinized saline was circulated for 4 h at a flow rate of 200 ml/min through the blood circuit. During the circulation, the dialysate did not flow on the dialysate side of the dialyzer. Samples were collected every hour during the circulation. Immediately after each sampling, the expression of P-selectin on the platelet surface was measured by its reaction with an anti-CD62P antigen conjugated with phycoerythrin (BioCytex, Marseille, France), as described above. PRP or LPRP prepared from the same blood was divided into two portions; one portion was circulated through a vitamin E-coated dialyzer and the other through a non-coated dialyzer. The percentage of activated platelets was determined as the percentage of platelets expressing P-selectin, detected by its reaction with the anti-CD62P antigen. Increase in platelet activation after circulation through the dialysis membrane was evaluated by subtracting the percentage of activated platelets in the control PRP stored at 37 °C in a water bath at each time point from that of the platelets in PRP circulated through the dialysis membrane:

Table 3 Technical data on dialyzer used

Dialyzer	APS-15MD	VPS-13H
Hollow fiber material	Polysulfone	Vitamin E-coated polysulfone
Inner diameter of hollow fibers (μm)	200	200
Membrane thickness (μm)	45	45
Number of hollow fibers	9,000	8,700
Effective hollow fiber length (mm)	266	241

$$\text{Increase in the ratio of platelets expressing P - selectin (\%)} = \frac{P_d}{N_d} \times 100 - \frac{P_c}{N_c} \times 100$$

where N is the total platelet number (set at 10,000 for forward and side scattering in the flow cytometry protocol), P is the number of platelets expressing P-selectin, subscript c is PRP stored at 37 °C, and subscript d is PRP coming in contact with the dialysis membrane. The calculated ratio represents the ratio of platelets expressing P-selectin in the PRP or LPRP circulating through the dialyzer.

Preparation of oxidized vitamin E-coated surface

Vitamin E (α-tocopherol, Wako Pure Chemical Industries, Ltd.) dissolved in ethanol at a concentration of 100 mg/ml was placed in some wells of a 96-well microplate (made of polypropylene) to prepare a vitamin E-coated surface. We did not use any method to bind the vitamin E chemically to the microplate surface. The vitamin E was fixed to the microplate surface via a hydrophobic interaction. Based on the eluted amount of vitamin E, the coated vitamin E was calculated to amount to approximately 0.2 mg/well. The density of vitamin E is 0.95 g/ml, and the surface area of a single microplate well is 32 mm^2, so the thickness of the coating was calculated to be 6.6 μm, meaning that a sufficient amount of vitamin E covered the surface of the microplate. The vitamin E coating conditions differed somewhat between the microplates and the dialysis membranes, although vitamin E fixed to both surfaces via a hydrophobic interaction: The amount of coated vitamin E on the microplate was larger than that on the dialysis membrane to minimize the effect of the base material (polypropylene) in the microplate experiment; almost all the vitamin E on the microplate was oxidized, unlike the vitamin E-coated membrane. A vitamin E-coated surface and an oxidized vitamin E-coated surface were used to distinguish the effects of oxidized vitamin E on platelet activation. Vitamin E and α-tocopherylquinone (the main oxidant end product of vitamin E) are insoluble in aqueous solution. Therefore, the effects of oxidized vitamin E-coated surfaces, but not oxidized vitamin E dissolved in an aqueous phase, on platelet activation can be examined.

Two microplates were prepared: one microplate was used for preparing the oxidized vitamin E-coated surface and the other for preparing the non-oxidized vitamin E-coated surface. To prepare the oxidized vitamin E-coated surface, vitamin E-coated wells were filled with 30 % hydrogen peroxide for a few minutes to prepare a wet surface, then the vitamin-E coating was irradiated overnight with ultraviolet (UV) light. The hydrogen peroxide solution was emptied prior to the UV irradiation to enhance the UV light exposure. We used hydrogen peroxide and UV irradiation to oxidize the vitamin E. Vitamin E was oxidized by hydroxyl radicals [46], which were made using hydrogen peroxide and UV irradiation [47]. The time of irradiation was determined so as to enable a sufficiently oxidized surface, which was confirmed by a ferric reducing antioxidant power (FRAP) assay (described below).

After the wells had been rinsed several times with saline, PRP was placed in the treated (oxidized vitamin E-coated surface) and untreated (vitamin E-coated) wells of the microplate. The superoxide anion concentration and expression of P-selectin on the platelet surface in the PRP were measured (described above). To confirm that the surface was actually oxidized, the coated vitamin E was redissolved in ethanol, and the change in absorbance was measured. We used non-treated vitamin E and D-α-tocopherylquinone (purity >97.0 %, Tokyo Chemical Industry Co., Ltd., Tokyo, Japan), the main oxidized end product of vitamin E, as negative and positive control, respectively.

Antioxidant capacity measured by the ferric reducing antioxidant power (FRAP) assay

Ferric reducing antioxidant power (FRAP) assay, which has been reported to be suitable for assessment of the antioxidant capacity of vitamin E-coated dialyzers [48], was used to examine the change in the antioxidant capacity of a vitamin E-coated membrane or vitamin E-coated surface. In the FRAP method, ferric ions (Fe^{3+}) are reduced to ferrous ions (Fe^{2+}) in acetate buffer by antioxidant activity. The ferrous ions were detected with 2,4,6-tripyridyl-s-triazine (TPTZ). TPTZ solution was prepared by dissolving 50 mg TPTZ in 12 N HCl (200 μl), then adding acetate buffer (2.46 g/l sodium acetate, 15 mL/l glacial acetic acid) to adjust the concentration (1.0 g TPTZ/l). Ferric ion solution (5.0 g $FeCl_3$/l) was prepared by dissolving $FeCl_3$ in acetate buffer.

The antioxidant capacity of the membrane (dialyzer) was measured in a single-pass flow-through mode. The dialyzer was primed with 2 l of saline and then substituted with acetate buffer. Then, the ferric ion solution was circulated through the dialyzer at a flow rate of 200 ml/min. Samples were collected from the blood-side outlet of the dialyzer every 1 min for 10 min, every 2 min from 10 to 20 min and every 5 min after 20 min. Then the samples were 1:10 diluted with the ferric ion solution and mixed with the TPTZ solution (1:1 volume ratio, molar ratio of TPTZ: Fe^{3+} = 1:2). The absorbance at 593 nm was measured with a spectrophotometer (V-530, JASCO, Tokyo, Japan). The absorbance was calibrated using $FeSO_4$ (Wako Pure Chemical Industries, Ltd.) solution.

The antioxidant capacity of the oxidized vitamin E-coated surface was measured by the same protocol. Ferric solution (5.0 g $FeCl_3$/l) was added to the vitamin E-coated microplate or oxidized vitamin E-coated microplate. After 1 min of incubation, a sample was collected

and 1:5–1:10 diluted (depending on Fe^{2+} concentration) with the ferric ion solution and mixed with TPTZ solution (1.0 g TPTZ/l) (1:1 volume ratio). The absorbance at 593 nm was measured with the spectrophotometer.

Generation of reactive oxygen species (ROS) in platelets adhering to the surface of the oxidized vitamin E-coated surface observed under a microscope

Glass-bottom culture dishes (35 mm) were coated with vitamin E, and oxidized and non-oxidized vitamin E-coated surfaces were prepared by the method described above. Then, 2 μl of aminophenyl fluorescein (APF, Sekisui Chemical, Tokyo, Japan) was added to 1 ml of PRP (final concentration 10 μM), followed by incubation of the mixture on an oxidized or non-oxidized vitamin E-coated surface for 20 min. APF was incorporated in the platelets during the incubation, and if highly reactive ROS such as hydroxyl radical, peroxynitrite, and hypochlorite were generated in the platelets, these ROS reacted with the APF to produce a fluorescent substance, fluorescein (excitation wavelength 490 nm, fluorescence wavelength 515 nm). After removal of the PRP and washing of the surface twice with saline, the platelets adhering to the surface were observed under a microscope (Axio Observer, Carl Zeiss AG, Oberkochen, Germany).

Statistical analysis

For the analyses of the superoxide anion production and P-selectin expression in the in vitro experiments performed using a microplate, the statistical significances of differences were determined by the Wilcoxon matched-pair signed-rank test. For the analysis of the PRP and LPRP circulation experiments through dialysis membranes, the statistical significances of differences were determined using an unpaired Student's *t* test. For the analysis of the results of the FRAP assay, the statistical significances of differences were determined by Bonferroni's post hoc test, which was used for multiple-group comparisons of the antioxidant capacity of dialyzers, and by an unpaired *t* test (Welch's *t* test) for the antioxidant capacity of oxidized vitamin E-coated surfaces. Differences with probability values (*P* value) of <0.05 were considered statistically significant.

Results

Superoxide anion production and P-selectin expression in PRP or LPRP after the addition of xanthine–xanthine oxidase or fMLP

The superoxide anion production level was measured in PRP and LPRP after the addition of xanthine–xanthine oxidase or fMLP (Fig. 1). Significant increases in the superoxide anion levels following the addition of xanthine oxidase were observed in the supernatants of both PRP and LPRP, with the levels returning to the baseline level following the addition of SOD. The degree of increase of the superoxide anion levels following the addition of xanthine–xanthine oxidase was the same in PRP and LPRP, indicating that no additional superoxide anions were produced by the leukocytes in LPRP.

Following the addition of fMLP, a leukocyte activator, the superoxide anion level in PRP not containing leukocytes did not change, whereas it significantly increased in LPRP, which contained leukocytes. This increase was also significantly suppressed by the addition of SOD.

The expression levels of P-selectin on the platelet surface were examined after the addition of xanthine–xanthine oxidase or fMLP to PRP and LPRP (Fig. 2). After the addition of xanthine–xanthine oxidase, a significant increase in the expression of P-selectin on the platelet surface was observed in both PRP and LPRP. Furthermore, this increase in the expression of P-selectin was significantly suppressed by the addition of SOD in both PRP and LPRP.

On the other hand, after the addition of fMLP, while a significant increase in the expression of P-selectin on the platelet surface was observed in LPRP, the platelet P-selectin expression level remained unchanged in PRP. With the addition of SOD, this increase in the expression of P-selectin in LPRP was significantly suppressed, indicating that the platelet activation in LPRP occurred as a result of leukocyte-generated superoxide anions.

Comparison of PRP and LPRP revealed increased platelet activation in LPRP, which was not suppressed by the addition of SOD (Fig. 2), indicating that another pathway besides superoxide anions, such as one involving platelet-activating factor (PAF), elastase or cathepsin G [37], mediated by leukocytes, might also be operative, at least in part, for the activation of platelets in the present experimental model.

Platelet activation during the circulation of PRP or LPRP through the dialysis membrane

The percentage of platelets expressing P-selectin increased with time, especially within the first 1 h, in each case. No significant difference was observed in the percentage of activated platelets between PRP and LPRP for a vitamin E-coated membrane (Fig. 3b). On the other hand, the percentage of activated platelets in LPRP that was circulated through the non-coated dialyzer was greater than that in PRP (the differences observed at 1, 2 and 4 h were significant) (Fig. 3c).

The antioxidant capacity of the dialysis membrane measured by FRAP assay was significantly decreased after

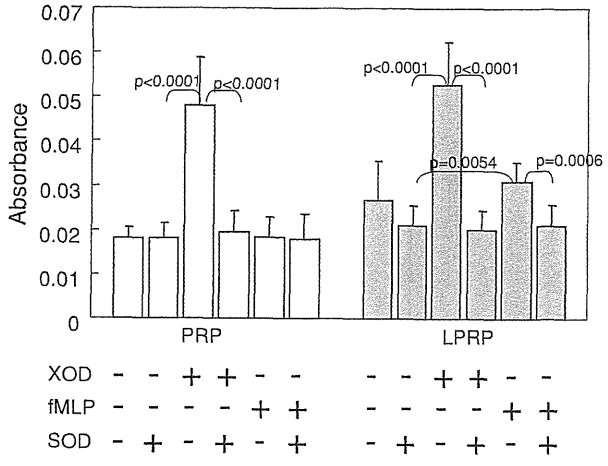

Fig. 1 Superoxide anion levels in PRP and LPRP following the addition of xanthine–xanthine oxidase (XOD) or fMLP with or without superoxide dismutase (SOD). *White bars* represent absorbance (reflecting the superoxide anion level) in PRP, and *gray bars* represent that in LPRP. Following the addition of xanthine–xanthine oxidase, a significant increase of the superoxide anion levels was observed in both PRP and LPRP. On the other hand, following the addition of fMLP, while the superoxide anion level in PRP remained unchanged, that in LPRP showed a significant increase. These increases were suppressed by the addition of SOD, indicating that the superoxide anions were actually produced in response to the addition of xanthine oxidase or fMLP. Data shown are the mean + SD ($n = 15$)

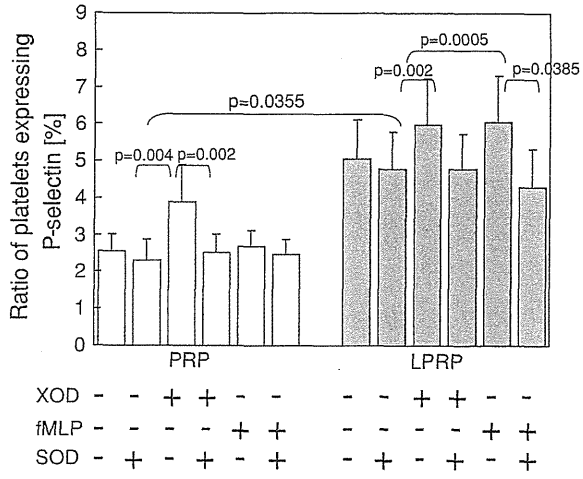

Fig. 2 P-selectin expression on the platelet surface in PRP or LPRP with the addition of xanthine–xanthine oxidase (XOD) or fMLP with or without superoxide dismutase (SOD). *White bars* represent the percentage of platelets expressing P-selectin on the platelets in PRP, and *gray bars* represent that in LPRP. Following the addition of xanthine–xanthine oxidase, a significant increase in the expression of P-selectin was observed in both PRP and LPRP. Following the addition of fMLP, while the expression on the platelets in PRP did not change, that in LPRP increased significantly. These increases were suppressed by the addition of SOD. A significant increase in platelet activation was also found following the addition of leukocytes to PRP not treated with XOD or fMLP. This increase was not suppressed by the addition of SOD. Data shown are the mean + SD ($n = 18$)

the membrane came in contact with PRP or LPRP; however, a high residual antioxidant capacity of the membrane still remained (Fig. 4). The residual antioxidant capacity of the membrane that was exposed to LPRP was significantly lower than that of the membrane exposed to PRP (Fig. 4).

Evaluation of the oxidized vitamin E-coated surface

To confirm that the surface of a microplate coated with vitamin E was oxidized after UV irradiation, the coated vitamin E was re-dissolved in ethanol, and the change in absorbance was measured for various concentrations (Fig. 5). The peak absorbances of vitamin E were obtained at 292 and 210–230 nm (Fig. 5a), while those of α-tocopherylquinone, the main oxidant end product of vitamin E, were obtained at 340, 264 and 210 nm (Fig. 5b). The peak absorbance of oxidized vitamin E was observed at 340 nm, and the absorbance at 264 nm was increased as compared with that of vitamin E (Fig. 5c); these absorbances corresponded to the peaks of α-tocopherylquinone. The oxidized surface was also evaluated by FRAP assay (Fig. 5d). The antioxidant capacity of the oxidized vitamin E-coated surface was significantly decreased as compared with that of the non-oxidized vitamin E-coated surface. The oxidized vitamin E-coated surface prepared by us was considered to be almost completely oxidized. However, the absorbances of the solution of re-dissolved oxidized vitamin E by ethanol showed the peaks of vitamin E (292 and 210–230 nm). This result was likely obtained because vitamin E was abundantly coated on the microplate, and the elution contained vitamin E present at the center of the vitamin E layer, which would not have been oxidized.

Superoxide anion level and platelet P-selectin expression in PRP placed in contact with non-oxidized vitamin E-coated and oxidized vitamin E-coated surface

The superoxide anion level and expression level of P-selectin on the platelets in PRP were measured after the PRP was placed in contact with a non-oxidized or oxidized vitamin E-coated surface. The superoxide anion level was greater in the PRP placed in contact with the oxidized vitamin E-coated surface than in the plasma placed in contact with the non-oxidized vitamin E-coated surface (Fig. 6a). P-selectin expression on the surface of the platelets was also higher in the PRP placed in contact with the oxidized vitamin E-coated surface than in that placed in contact with the non-oxidized vitamin E-coated surface (Fig. 6b).

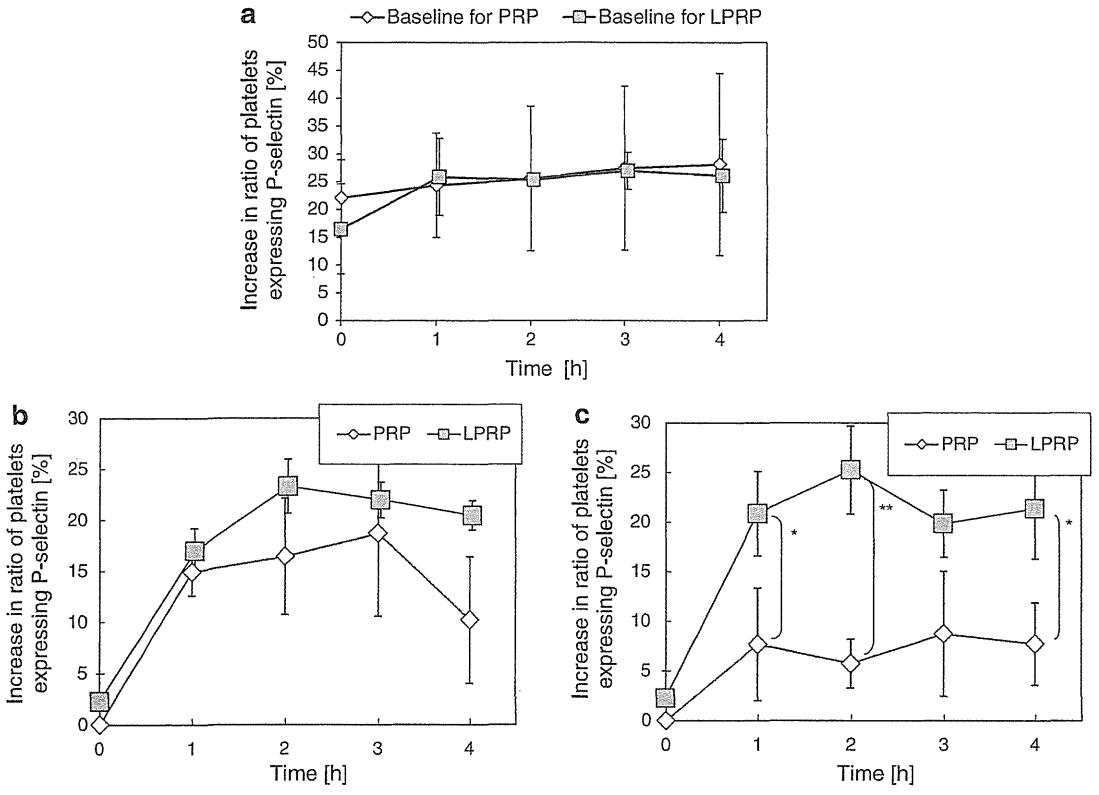

Fig. 3 Activation of platelets in PRP and LPRP during circulation for 4 h through a vitamin E-coated or non-coated dialysis membrane. **a** Baseline of platelet activation. The baseline was the percentage of platelets expressing P-selectin in PRP derived from the same blood incubated in a water bath at 37 °C for the same length of time. **b** and **c** Increase in the ratio of platelets expressing P-selectin for vitamin E-coated and non-coated membranes, respectively. P-selectin expression on the platelets in LPRP that came in contact with the vitamin E-coated membrane increased in the same manner. Platelets in LPRP that came in contact with the non-coated membrane showed a greater increase in the expression levels of P-selectin compared with those in PRP. Data shown are the mean ± SD ($n = 3$). *Asterisk* and *double asterisks* indicate significant difference ($P < 0.05$ and $P < 0.01$, respectively) between PRP and LPRP at the same time

Generation of ROS in the platelets adhering to the surface of the oxidized vitamin E-coated surface

Platelet aggregation was observed on the oxidized vitamin E-coated surface, whereas no platelet aggregation was observed on the non-oxidized vitamin E-coated surface (Fig. 7 left panels). ROS were generated in the platelets adhering to the oxidized vitamin E-coated surface, whereas few ROS were produced in the platelets adhering to the non-oxidized vitamin E-coated surface (Fig. 7 right panels).

Discussion

The new findings of this study include: (1) platelet activation triggered by leukocytes was suppressed in plasma coming in contact with a vitamin E-coated membrane because no difference was observed in platelet activation between PRP and LPRP, while paradoxically, the membrane itself directly induced platelet activation; (2) the vitamin E-coated surface became partially oxidized upon coming in contact with PRP or LPRP, but sufficient residual antioxidant capacity was maintained; (3) an oxidized vitamin E-coated surface induced activation of platelets.

We used isolated platelets and leukocytes to carry out the experiments under well-defined conditions suitable for examining the effects of using a vitamin E-coated surface on platelet activation. Since we used purchased porcine blood, the processes of blood withdrawal, transfer, isolation of the cells, and reconstitution of PRP or LPRP may prime or activate the platelets and/or leukocytes, which might inhibit the normal reactions of these cells. Before we examined the effect of using a vitamin E-coated surface, we confirmed that the platelet and leukocyte interactions were mediated by superoxide anions in this experimental model established using isolated platelets and leukocytes (Figs. 1, 2). The results obtained with the present model indicate that the superoxide anions generated by the

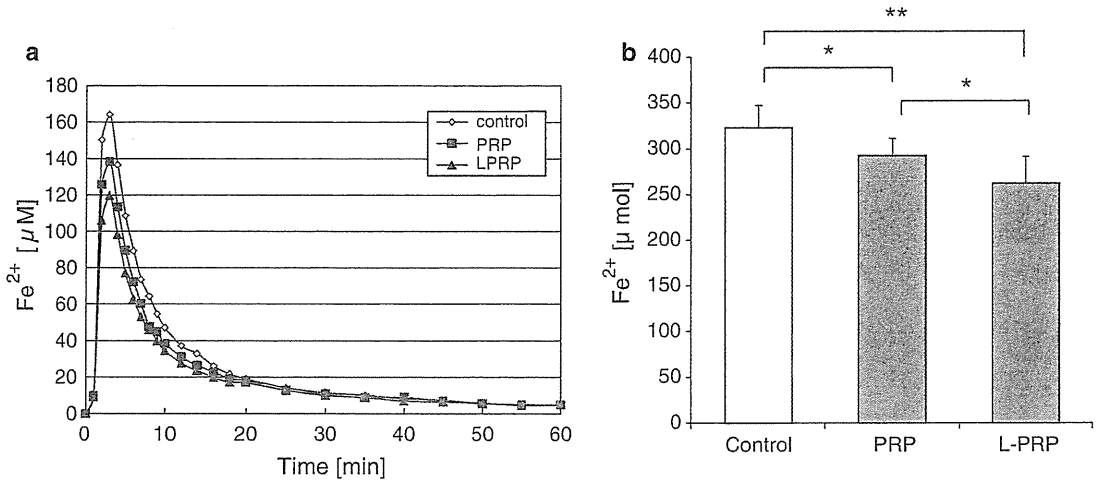

Fig. 4 Antioxidant capacity of a vitamin E-coated dialysis membrane measured by FRAP assay. After circulation of PRP or LPRP for 4 h through the dialyzer, a solution of ferric ions (Fe^{3+}) was circulated through the dialyzer at a flow rate of 200 ml/min. Then, the concentration of ferrous ions (Fe^{2+}) was measured by mixing samples collected from the blood-side outlet of the dialyzer solution with the TPTZ solution. **a** A typical Fe^{3+} reduction curve produced during the Fe^{3+} flow-though experiment. The area under the curve was calculated to determine the total antioxidant capacity. **b** The antioxidant capacity of the membrane measured by the FRAP assay was significantly decreased after the membrane came in contact with PRP or LPRP, although a residual antioxidant capacity of the membrane still remained. The residual antioxidant capacity of the membrane coming in contact with LPRP was significantly lower than that of the membrane coming in contact with PRP. Data shown are the mean + SD ($n = 7$). *Asterisk* and *double asterisks* indicate significant difference ($P < 0.05$ and $P < 0.01$, respectively)

activated leukocytes induce platelet activation, which was consistent with the results obtained from experiments using isolated platelets (PRP) from healthy volunteers [37], as well as whole blood [31]. Therefore, we concluded that the experimental model we used was valid for investigating the interactions among the coated vitamin E surface, platelets and leukocytes, especially in the context of the interactions involving superoxide anions.

Limitations of this study associated with the model employed were as follows: (1) We used PRP and LPRP derived from porcine whole blood instead of human blood, because a large amount of fresh blood was required to purify the PRP and LPRP needed to compare the vitamin E-coated and non-coated dialyzer membranes. The use of porcine blood might limit the direct application of the results to human blood. (2) We used PRP or LPRP rather than whole blood to focus on the mutual interactions among the vitamin E-coated surface, platelets and leukocytes. Therefore, additional investigations using whole blood containing erythrocytes are warranted, as well as those in clinical settings. (3) We adjusted the platelet and leukocyte concentrations in the PRP or LPRP to be approximately 50 % of the original blood concentrations, and the volume of the circulated test solution (1 l) was lower than that of blood in the body. The activity of the leukocytes (the ability to produce superoxide anions) might also be reduced, and no recruitment of fresh neutrophils from the bone marrow occurred in our system. Therefore, a vitamin E-coated membrane might be oxidized more extensively during clinical use. However, because high platelet activation did not occur under clinical conditions [27], the antioxidant capacity probably would remain sufficient during hemodialysis. Further study of the remaining antioxidant capacity of clinically used dialyzers is needed. (4) We used different-sized dialyzers. The contact times of the non-coated and the vitamin E-coated dialyzers at a flow rate of 200 ml/min were 22.6 and 19.8 s, and the wall shear rates were 472 and 488 s^{-1}, respectively; these differences did not seem to have a notable effect on platelet activation. However, these factors are known to affect platelet activation and might have affected platelet activation in this study. Therefore, we compared platelet activation mainly between PRP and LPRP for each membrane.

Our results indicated that the vitamin E-coated membrane suppressed platelet activation via leukocyte activation (Fig. 3b). Possible explanations for this deduction are: (1) the scavenging effect of the vitamin E-coated membrane for the superoxide anions produced by leukocytes and (2) the suppression of leukocyte stimulation by the dialysis membrane. However, the results also indicated that the vitamin E-coated membrane may directly induce platelet activation. Although vitamin E itself has an inhibitory effect on platelet activation [19–23], a vitamin E-coated membrane seemed to directly induce platelet activation. Therefore, we hypothesized that the platelet activation is related to oxidation of the vitamin E coating on the membrane surface.

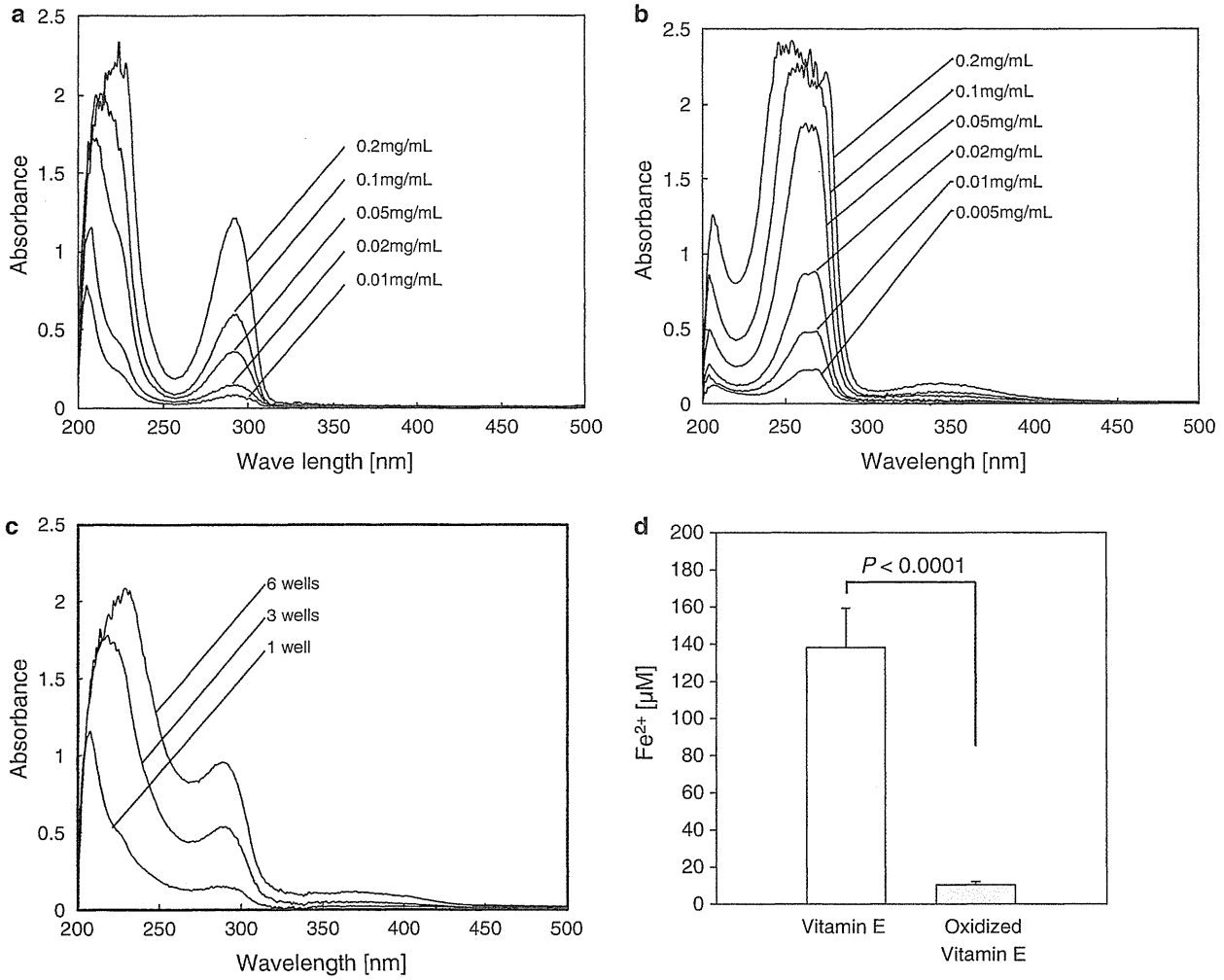

Fig. 5 Absorbance of the oxidized vitamin E coated on the surface. The coated vitamin E was re-dissolved in 10 ml of ethanol collected from 1, 3 or 6 wells of the microplate, and the absorbance of the solution was measured. **a** Absorbance of vitamin E used at different concentrations. Peak absorbance was observed at 292 and 210–230 nm. **b** Absorbance of α-tocopherylquinone, the main oxidant end products of vitamin E. Peak absorbance was observed at 340, 264 and 210 nm. **c** Absorbance of oxidized vitamin E. The absorbance of oxidized vitamin E was high at 340 and 264 nm. These *peaks* corresponded to the peaks of α-tocopherylquinone. **d** Antioxidant capacity measured by the FRAP assay. The antioxidant capacity of the oxidized vitamin E-coated surface was significantly decreased as compared with that of the non-oxidized vitamin E-coated surface. Data shown are the mean + SD ($n = 10$)

We then examined the activation of platelets in the plasma coming in contact with the oxidized vitamin E-coated surface. The superoxide anion concentration and P-selectin expression on the platelets in PRP increased when the PRP was placed in contact with the oxidized vitamin E-coated surface (Fig. 6). Platelet aggregation and ROS production in the adherent platelets were actually pronounced on the oxidized surface (Fig. 7). It has been reported that platelet activation by superoxide anions may be enhanced in a paracrine as well as autocrine manner [49, 50]. Therefore, these results can be attributed to: (1) a decrease in the scavenging effect of the oxidized surface and/or (2) direct activation of platelets by the oxidized surface. The antioxidant capacity of a dialysis membrane measured by the FRAP assay was significantly decreased after the membrane came in contact with PRP or LPRP; however, the total antioxidant capacity still remained high, even after 4 h circulation (Fig. 4). Therefore, we considered that platelet activation after the plasma came in contact with the oxidized vitamin E-coated surface mainly occurred because of direct activation of the platelets by the oxidized surface rather than being a result of a decrease in the total scavenging effect of the oxidized surface.

The activation trigger was considered to be different between the two types of membranes: Platelet activation on

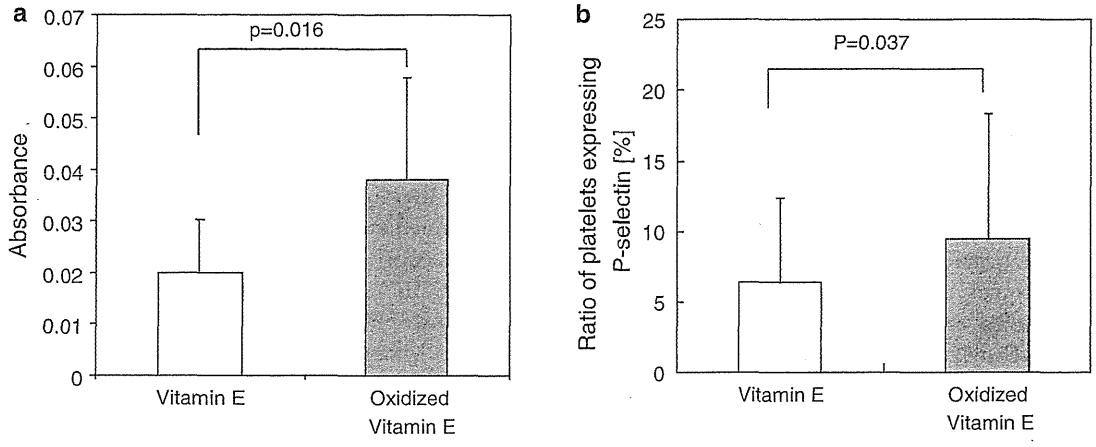

Fig. 6 Superoxide anion levels and platelet P-selectin expression in PRP coming in contact with a non-oxidized vitamin E-coated surface or oxidized vitamin E-coated surface. **a** Superoxide anion level. **b** P-selectin expression on the platelet surface. *White bars* represent superoxide anion levels or platelet P-selectin expression in PRP placed in contact with the non-oxidized vitamin E-coated surface, and *gray bars* represent the results in PRP placed in contact with the oxidized vitamin E-coated surface. Both the superoxide anion levels in PRP and the platelet P-selectin expression were greater in the PRP placed in contact with the oxidized vitamin E-coated surface than in that placed in contact with the non-oxidized vitamin E-coated surface. Data shown are the mean + SD ($n = 10$)

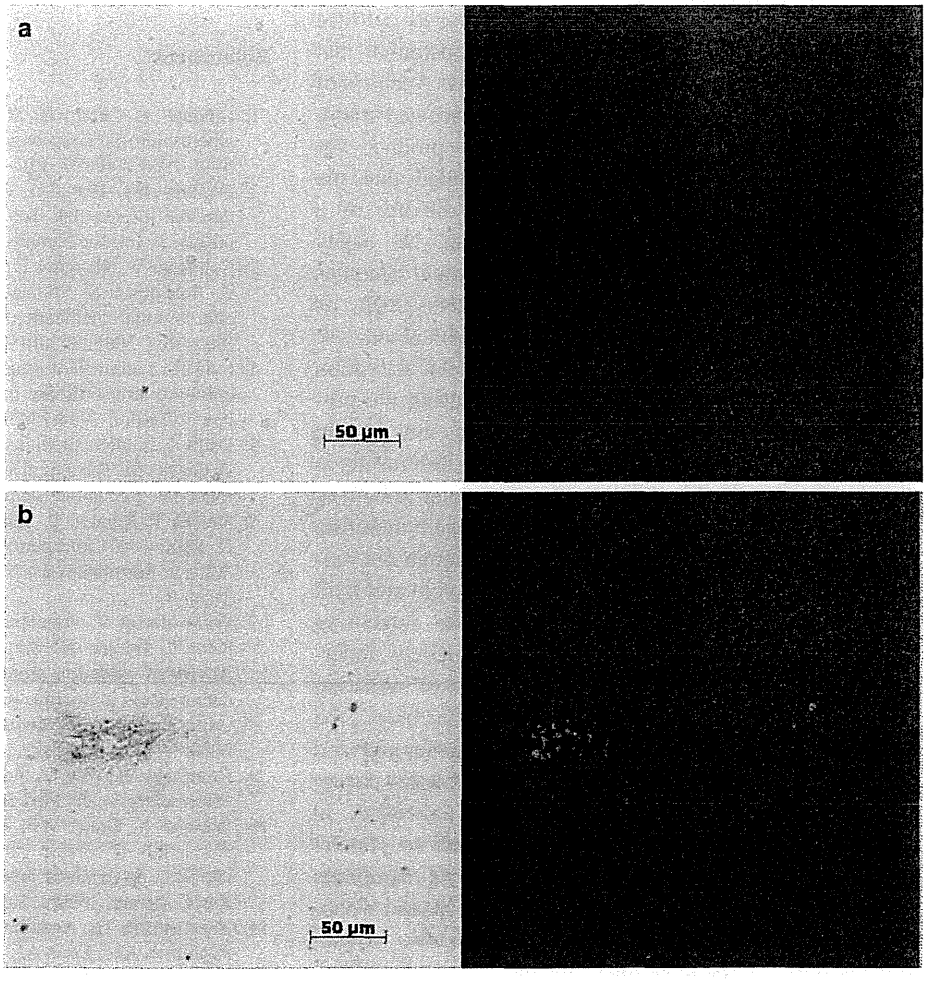

Fig. 7 Platelet aggregation and platelet production of ROS in PRP upon contact with an oxidized vitamin E-coated surface. **a** Platelets on the non-oxidized vitamin E-coated surface, **b** platelets on the oxidized vitamin E-coated surface. *Left panels* represent typical light-field images of platelets on the surface, and *right panels* represent the corresponding fluorescent images. After incubation of PRP on the membrane surface for 20 min, the PRP was washed off by saline, and the adherent platelets were examined. Platelet aggregation was observed on the oxidized vitamin E-coated surface, whereas no platelet aggregation was observed on the non-oxidized vitamin E-coated surface. Reactive oxygen species (ROS) were produced in the platelets adhering to the oxidized vitamin E-coated surface, whereas no ROS production was observed in the platelets adhering to the non-oxidized vitamin E-coated surface; the ROS production was detected by aminophenyl fluorescein

the vitamin E-coated membrane was considered to be a result of direct interaction of the platelets with the oxidized vitamin E-coated membrane, while the platelet activation on the non-coated membrane was considered to be attributable to leukocyte activation and leukocyte-produced superoxide anions. The platelet activation by oxidized vitamin E on the vitamin E-coated membrane, which increased with time during dialysis, could be the reason why a distinct beneficial effect of vitamin E-coating of dialysis membranes on platelet activation could not be clearly appreciated in the clinical setting. Since activated platelets induce leukocyte activation [32–34, 51], both activated leukocyte-produced and activated platelet-produced superoxide anions induce platelet activation in an autocrine manner in a positive feedback loop, as shown in the present study.

Using the FRAP assay, we determined the antioxidant capacity of the vitamin E coating on the microplate surface (Fig. 5). It was found that the antioxidant capacity of the coated surface greatly decreased. P-selectin expression on the platelets in PRP increased when the PRP was placed in contact with the oxidized vitamin E-coated surface (Fig. 6). These experiments clearly demonstrated that oxidized vitamin E actually activates platelets. Analysis of the end products of the oxidized vitamin E-coated membrane revealed that the main oxidation end product was α-tocopherylquinone [48]. The results implied that the reduced platelet activation observed with the use of a vitamin E-coated dialysis membrane can be easily enhanced if the vitamin E-coated membrane becomes oxidized to yield oxidation end products such as α-tocopherylquinone after coming in contact with blood. Use of a vitamin E-coated surface can reduce platelet activation mediated by superoxide anions; however, during the process of reduction of the superoxide anions, the vitamin E-coated surface becomes oxidized, which in turn results in direct activation of the platelets. The beneficial effects of vitamin E with respect to platelet activation were therefore counteracted by the oxidized vitamin E, although the oxidation of other blood components, such as protein and lipid oxidations, would still be inhibited by the remaining scavenging capacity of the membrane. If a patient undergoing hemodialysis has sufficient amounts of reducing substances, such as ascorbic acid, in his or her blood, the vitamin E radical would be sufficiently regenerated and would be unlikely to form oxidation end products during hemodialysis, thereby suppressing platelet activation. In this case, the beneficial effects, with respect to platelet activation, of using a vitamin E-coated dialysis membrane would be more pronounced; otherwise, they would disappear. If a patient's antioxidant capacity is low, supplementation with a reducing agent for the vitamin E radical, such as ascorbic acid, during hemodialysis therapy could be a new option for maximizing the beneficial effects of vitamin E coating.

In summary, vitamin E-coating of the surface of a dialysis membrane reduced the platelet activation mediated by superoxide anions, presumably because of the reduction of superoxide anions by the vitamin E; however, during the process, the vitamin E-coated surface itself became oxidized, which induced platelet activation. Thus, the beneficial effects of the vitamin E-coated dialysis membrane in respect to the platelet activation were counterbalanced by the effects of oxidized vitamin E. This could explain why use of a vitamin E-coated dialysis membrane does not appear to reduce platelet activation in the clinical setting.

Acknowledgments The dialyzers used in the present study were kindly supplied by Asahi Kasei Kuraray Medical, Tokyo, Japan. This work was partly supported by research funding from Asahi Kasei Kuraray Medical Co., Ltd., to H. K. and K. K.

Conflict of interest There are no other conflicts of interests to declare in respect of this manuscript.

References

1. Lindner A, Charra B, Sherrard DJ, Scribner BH. Accelerated atherosclerosis in prolonged maintenance hemodialysis. N Engl J Med. 1974;290:697–701.
2. O'Hare AM, Hsu CY, Bacchetti P, Johansen KL. Peripheral vascular disease risk factors among patients undergoing hemodialysis. J Am Soc Nephrol. 2002;13:497–503.
3. Campean V, Neureiter D, Varga I, Runk F, Reiman A, Garlichs C, Achenbach S, Nonnast-Daniel B, Amann K. Atherosclerosis and vascular calcification in chronic renal failure. Kidney Blood Press Res. 2005;28:280–9.
4. Lam JY, Latour JG, Lesperance J, Waters D. Platelet aggregation, coronary artery disease progression and future coronary events. Am J Cardiol. 1994;73:333–8.
5. Daub K, Lindemann S, Langer H, Seizer P, Stellos K, Siegel-Axel D, Gawaz M. The evil in atherosclerosis: adherent platelets induce foam cell formation. Semin Thromb Hemost. 2007;33:173–8.
6. Sanaka T, Higuchi C, Shinobe T, Nishimura H, Omata M, Nihei H, Sugino N. Lipid peroxidation as an indicator of biocompatibility in haemodialysis. Nephrol Dial Transplant. 1995;10(Suppl 3):34–8.
7. Witko-Sarsat V, Friedlander M, Capeillere-Blandin C, Nguyen-Khoa T, Nguyen AT, Zingraff J, Jungers P, Descamps-Latscha B. Advanced oxidation protein products as a novel marker of oxidative stress in uremia. Kidney Int. 1996;49:1304–13.
8. Galli F, Ronco C. Oxidant stress in hemodialysis. Nephron. 2000;84:1–5.
9. Esterbauer H, Wag G, Puhl H. Lipid peroxidation and its role in atherosclerosis. Br Med Bull. 1993;49:566–76.
10. Schmidt K, Graier WF, Kostner GM, Mayer B, Kukovetz WR. Activation of soluble guanylate cyclase by nitrovasodilators is inhibited by oxidized low-density lipoprotein. Biochem Biophys Res Commun. 1990;172:614–9.
11. Rajavashisth TB, Andalibi A, Territo MC, Berliner JA, Navab M, Fogelman AM, Lusis AJ. Induction of endothelial cell expression of granulocyte and macrophage colony-stimulating factors by modified low-density lipoproteins. Nature. 1990;344:254–7.

12. Leake DS. Effects of mildly oxidized low-density lipoprotein on endothelial cell function. Curr Opin Lipidol. 1991;2:306–10.
13. Orekhov AN. Lipoprotein immune complexes and their role in atherogenesis. Curr Opin Lipidol. 1991;2:329–33.
14. Quinn MT, Parthasarathy S, Fong LG, Steinberg D. Oxidatively modified low density lipoproteins: a potential role in recruitment and retention of monocyte/macrophages during atherogenesis. Proc Natl Acad Sci USA. 1987;84:2995–8.
15. Aggarwal A, Kabbani SS, Rimmer JM, Gennari FJ, Taatjes DJ, Sobel BE, Schneider DJ. Biphasic effects of hemodialysis on platelet reactivity in patients with end-stage renal disease: a potential contributor to cardiovascular risk. Am J Kidney Dis. 2002;40:315–22.
16. Thaulow E, Erikssen J, Sandvik L, Stormorken H, Cohn PF. Blood platelet count and function are related to total and cardiovascular death in apparently healthy men. Circulation. 1991;84:613–7.
17. Trip MD, Cats VM, van Capelle FJ, Vreeken J. Platelet hyperreactivity and prognosis in survivors of myocardial infarction. N Engl J Med. 1990;322:1549–54.
18. Pascoe GA, Olafsdottir K, Reed DJ. Vitamin E protection against chemical-induced cell injury. I. Maintenance of cellular protein thiols as a cytoprotective mechanism. Arch Biochem Biophys. 1987;256:150–8.
19. Freedman JE, Farhat JH, Loscalzo J, Keaney JF Jr. Alpha-tocopherol inhibits aggregation of human platelets by a protein kinase c-dependent mechanism. Circulation. 1996;94:2434–40.
20. Keaney JF, Jr., Simon DI, Freedman JE. Vitamin E and vascular homeostasis: implications for atherosclerosis. FASEB J. 1999;13:965–75.
21. Azzi A, Breyer I, Feher M, Pastori M, Ricciarelli R, Spycher S, Staffieri M, Stocker A, Zimmer S, Zingg JM. Specific cellular responses to alpha-tocopherol. J Nutr. 2000;130:1649–52.
22. Freedman JE, Keaney JF Jr. Vitamin E inhibition of platelet aggregation is independent of antioxidant activity. J Nutr. 2001;131:374S–7S.
23. Liu M, Wallmon A, Olsson-Mortlock C, Wallin R, Saldeen T. Mixed tocopherols inhibit platelet aggregation in humans: potential mechanisms. Am J Clin Nutr. 2003;77:700–6.
24. Sasaki M. Development of vitamin E-modified polysulfone membrane dialyzers. J Artif Organs. 2006;9:50–60.
25. Calo LA, Naso A, Pagnin E, Davis PA, Castoro M, Corradin R, Riegler P, Cascone C, Huber W, Piccoli A. Vitamin E-coated dialyzers reduce oxidative stress related proteins and markers in hemodialysis—a molecular biological approach. Clin Nephrol. 2004;62:355–61.
26. Morimoto H, Nakao K, Fukuoka K, Sarai A, Yano A, Kihara T, Fukuda S, Wada J, Makino H. Long-term use of vitamin E-coated polysulfone membrane reduces oxidative stress markers in haemodialysis patients. Nephrol Dial Transplant. 2005;20:2775–82.
27. Clermont G, Lecour S, Cabanne JF, Motte G, Guilland JC, Chevet D, Rochette L. Vitamin E-coated dialyzer reduces oxidative stress in hemodialysis patients. Free Radic Biol Med. 2001;31:233–41.
28. Satoh M, Yamasaki Y, Nagake Y, Kasahara J, Hashimoto M, Nakanishi N, Makino H. Oxidative stress is reduced by the long-term use of vitamin E-coated dialysis filters. Kidney Int. 2001;59:1943–50.
29. Sosa MA, Balk EM, Lau J, Liangos O, Balakrishnan VS, Madias NE, Pereira BJ, Jaber BL. A systematic review of the effect of the Excebrane dialyser on biomarkers of lipid peroxidation. Nephrol Dial Transplant. 2006;21:2825–33.
30. Bazzoni G, Dejana E, Del Maschio A. Platelet–neutrophil interactions. Possible relevance in the pathogenesis of thrombosis and inflammation. Haematologica. 1991;76:491–9.
31. Li N, Hu H, Lindqvist M, Wikstrom-Jonsson E, Goodall AH, Hjemdahl P. Platelet–leukocyte cross talk in whole blood. Arterioscler Thromb Vasc Biol. 2000;20:2702–8.
32. Nagata K, Tsuji T, Todoroki N, Katagiri Y, Tanoue K, Yamazaki H, Hanai N, Irimura T. Activated platelets induce superoxide anion release by monocytes and neutrophils through P-selectin (CD62). J Immunol. 1993;151:3267–73.
33. Nagata K, Tsuji T, Hanai N, Irimura T. Role of O-linked carbohydrate chains on leukocyte cell membranes in platelet-induced leukocyte activation. J Biol Chem. 1994;269:23290–5.
34. Tsuji T, Nagata K, Koike J, Todoroki N, Irimura T. Induction of superoxide anion production from monocytes an neutrophils by activated platelets through the P-selectin-sialyl Lewis X interaction. J Leukoc Biol. 1994;56:583–7.
35. Bath PM, Hassall DG, Gladwin AM, Palmer RM, Martin JF. Nitric oxide and prostacyclin. Divergence of inhibitory effects on monocyte chemotaxis and adhesion to endothelium in vitro. Arterioscler Thromb. 1991;11:254–60.
36. Gamble JR, Skinner MP, Berndt MC, Vadas MA. Prevention of activated neutrophil adhesion to endothelium by soluble adhesion protein GMP140. Science. 1990;249:414–7.
37. Salvemini D, de Nucci G, Sneddon JM, Vane JR. Superoxide anions enhance platelet adhesion and aggregation. Br J Pharmacol. 1989;97:1145–50.
38. Salvemini D, de Nucci G, Gryglewski RJ, Vane JR. Human neutrophils and mononuclear cells inhibit platelet aggregation by releasing a nitric oxide-like factor. Proc Natl Acad Sci USA. 1989;86:6328–32.
39. Zatta A, Prosdocimi M, Bertele V, Bazzoni G, Del Maschio A. Inhibition of platelet function by polymorphonuclear leukocytes. J Lab Clin Med. 1990;116:651–60.
40. Burton GW, Doba T, Gabe EJ, Hughes L, Lee FL, Prasad L, Ingold KU. Autoxidation of biological molecules. 4. Maximizing the antioxidant activity of phenols. J Am Chem Soc. 1985;107:7053–65.
41. Niki E. Antioxidants in relation to lipid peroxidation. Chem Phys Lipids. 1987;44:227–53.
42. Barclay LRC. 1992 syntex award lecture model biomembranes: quantitative studies of peroxidation, antioxidant action, partitioning, and oxidative stress. Can J Chem. 1993;71:1–16.
43. Mukai K, Ouchi A, Mitarai A, Ohara K, Matsuoka C. Formation and decay dynamics of vitamin E radical in the antioxidant reaction of vitamin E. Bull Chem Soc Jpn. 2009;82:494–503.
44. Liebler DC, Burr JA. Oxidation of vitamin E during iron-catalyzed lipid peroxidation: evidence for electron-transfer reactions of the tocopheroxyl radical. Biochemistry. 1992;31:8278–84.
45. Ukeda H, Kawana D, Maeda S, Sawamura M. Spectrophotometric assay for superoxide dismutase based on the reduction of highly water-soluble tetrazolium salts by xanthine–xanthine oxidase. Biosci Biotechnol Biochem. 1999;63:485–8.
46. Navarrete M, Rangel C, Corchado JC, Espinosa-García J. Trapping of the OH radical by alpha-tocopherol: a theoretical study. J Phys Chem A. 2005;109:4777–84.
47. von Sonntag C. Advanced oxidation processes: mechanistic aspects. Water Sci Technol. 2008;58:1015–21.
48. Floridi A, Piroddi M, Pilolli F, Matsumoto Y, Aritomi M, Galli F. Analysis method and characterization of the antioxidant capacity of vitamin E-interactive polysulfone hemodialyzers. Acta Biomater. 2009;5:2974–82.
49. Arthur JF, Gardiner EE, Kenny D, Andrews RK, Berndt MC. Platelet receptor redox regulation. Platelets. 2008;19:1–8.
50. Del Principe D, Frega G, Savini I, Catani MV, Rossi A, Avigliano L. The plasma membrane redox system in human platelet functions and platelet–leukocyte interactions. Thromb Haemost. 2009;101:284–9.
51. Itoh S, Susuki C, Tsuji T. Platelet activation through interaction with hemodialysis membranes induces neutrophils to produce reactive oxygen species. J Biomed Mater Res A. 2006;77:294–303.